

# THE GREEN FLUORESCENT PROTEIN

*Roger Y. Tsien*

Howard Hughes Medical Institute; University of California, San Diego; La Jolla,  
CA 92093-0647

KEY WORDS: *Aequorea*, mutants, chromophore, bioluminescence, GFP

---

## ABSTRACT

In just three years, the green fluorescent protein (GFP) from the jellyfish *Aequorea victoria* has vaulted from obscurity to become one of the most widely studied and exploited proteins in biochemistry and cell biology. Its amazing ability to generate a highly visible, efficiently emitting internal fluorophore is both intrinsically fascinating and tremendously valuable. High-resolution crystal structures of GFP offer unprecedented opportunities to understand and manipulate the relation between protein structure and spectroscopic function. GFP has become well established as a marker of gene expression and protein targeting in intact cells and organisms. Mutagenesis and engineering of GFP into chimeric proteins are opening new vistas in physiological indicators, biosensors, and photochemical memories.

---

## CONTENTS

NATURAL AND SCIENTIFIC HISTORY OF GFP .....	510
<i>Discovery and Major Milestones</i> .....	510
<i>Occurrence, Relation to Bioluminescence, and Comparison with         Other Fluorescent Proteins</i> .....	511
PRIMARY, SECONDARY, TERTIARY, AND QUATERNARY STRUCTURE .....	512
<i>Primary Sequence from Cloning</i> .....	512
<i>Crystal Structures; Tolerance of Truncations</i> .....	515
<i>Dimerization</i> .....	515
ABSORBANCE AND FLUORESCENCE PROPERTIES .....	518
<i>Classification of GFPs</i> .....	518
<i>General Relation of Structure to Spectra</i> .....	525
<i>Two-Photon Excitation</i> .....	526
<i>Effects of pH</i> .....	527
<i>Effects of Temperature and Protein Concentrations</i> .....	527

<i>Effects of Prior Illumination</i> .....	527
EXPRESSION, FORMATION, MATURATION, RENATURATION, AND OBSERVATION .....	529
<i>Promoters, Codon Usage, and Splicing</i> .....	529
<i>Folding Mutations and Thermotolerance</i> .....	530
<i>Requirement for O<sub>2</sub></i> .....	530
<i>Histology in Fixed Tissues</i> .....	532
PASSIVE APPLICATIONS OF GFP .....	532
<i>Reporter Gene, Cell Marker</i> .....	532
<i>Fusion Tag</i> .....	533
GFP AS AN ACTIVE INDICATOR .....	534
<i>Protease Action</i> .....	535
<i>Transcription Factor Dimerization</i> .....	535
<i>Ca<sup>2+</sup> Sensitivity</i> .....	536
<i>What Are the Best FRET Partners?</i> .....	538
OUTLOOK FOR FUTURE RESEARCH .....	539
<i>Cloning of Related GFPs</i> .....	539
<i>Protein Folding and Chromophore Folding</i> .....	539
<i>Altered Wavelengths of Fluorescence</i> .....	539
<i>Altered Chemical and Photochemical Sensitivities</i> .....	540
<i>Fusions Other Than at N- or C-Terminus</i> .....	540
<i>Alternatives to Fluorescence</i> .....	540

## NATURAL AND SCIENTIFIC HISTORY OF GFP

### *Discovery and Major Milestones*

Green Fluorescent Protein was discovered by Shimomura et al (1) as a companion protein to aequorin, the famous chemiluminescent protein from *Aequorea* jellyfish. In a footnote to their account of aequorin purification, they noted that “a protein giving solutions that look slightly greenish in sunlight through only yellowish under tungsten lights, and exhibiting a very bright, greenish fluorescence in the ultraviolet of a Mineralite, has also been isolated from squeezates.” This description of the appearance of GFP solutions is still accurate. The same group (2) soon published the emission spectrum of GFP, which peaked at 508 nm. They noted that the green bioluminescence of living *Aequorea* tissue also peaked near this wavelength, whereas the chemiluminescence of pure aequorin was blue and peaked near 470 nm, which was close to one of the excitation peaks of GFP. Therefore the GFP converted the blue emission of aequorin to the green glow of the intact cells and animals. Morin & Hastings (3) found the same color shift in the related coelenterates *Obelia* (a hydroid) and *Renilla* (a sea pansy) and were the first to suggest radiationless energy transfer as the mechanism for exciting coelenterate GFPs *in vivo*. Morise et al (4) purified and crystallized GFP, measured its absorbance spectrum and fluorescence quantum yield, and showed that aequorin could efficiently transfer its luminescence energy to GFP when the two were coadsorbed onto a cationic support. Prendergast & Mann (5) obtained the first clear estimate for the

monomer molecular weight. Shimomura (6) proteolyzed denatured GFP, analyzed the peptide that retained visible absorbance, and correctly proposed that the chromophore is a 4-(*p*-hydroxybenzylidene)imidazolidin-5-one attached to the peptide backbone through the 1- and 2-positions of the ring.

*Aequorea* and *Renilla* GFPs were later shown to have the same chromophore (7); and the pH sensitivity, aggregation tendency (8), and renaturation (9) of *Aequorea* GFP were characterized. But the crucial breakthroughs came with the cloning of the gene by Prasher et al (10) and the demonstrations by Chalfie et al (11) and Inouye & Tsuji (12) that expression of the gene in other organisms creates fluorescence. Therefore the gene contains all the information necessary for the posttranslational synthesis of the chromophore, and no jellyfish-specific enzymes are needed.

### *Occurrence, Relation to Bioluminescence, and Comparison with Other Fluorescent Proteins*

Green fluorescent proteins exist in a variety of coelenterates, both hydrozoa such as *Aequorea*, *Obelia*, and *Phialidium*, and anthozoa such as *Renilla* (3, 13). In this review, GFP refers to the *Aequorea* protein except where another genus name is specifically indicated. These GFPs seem to be partners with chemiluminescent proteins and to control the color of the emission in vivo. Despite interesting speculations, it remains unclear why these coelenterates glow, why green emission should be ecologically so superior to the blue of the primary emitters, and why the animals synthesize a separate GFP rather than mutate the chemiluminescent protein to shift its wavelengths. Other than *Aequorea* GFP, only *Renilla* GFP has been biochemically well characterized (14). Despite the apparent identity of the core chromophore in *Renilla* and *Aequorea* GFP, *Renilla* GFP has a much higher extinction coefficient, resistance to pH-induced conformational changes and denaturation, and tendency to dimerize (7).

Unfortunately, *Aequorea* GFP genes are the only GFP genes that have been cloned. Several other bioluminescent species also have emission-shifting accessory proteins, but so far the chromophores all seem to be external cofactors such as lumazines (15) or flavins (16), which diminish their attractiveness as biotechnological tags and probes. Likewise phycobiliproteins (17) and peridinin-chlorophyll-*a* protein (18), which are highly fluorescent and attractively long-wavelength accessory pigments in photosynthesis, use tetrapyrrole cofactors as their pigments. Correct insertion of the cofactors into the apoproteins has not been demonstrated in foreign organisms, so these proteins are not ready to compete with *Aequorea* GFP. A variety of marine organisms fluoresce, but the biochemistry of the fluorophores is almost completely unknown. Painstaking research like that undertaken by the pioneers of *Aequorea* and *Renilla* GFP would be needed before cloning efforts could begin. It is unclear

whether any investigators or granting agencies are still patient enough to undertake and fund such long-term groundwork.

## PRIMARY, SECONDARY, TERTIARY, AND QUATERNARY STRUCTURE

### *Primary Sequence from Cloning*

The sequence of wild-type *Aequorea* GFP (10) is given in Figure 1. Sequences of at least four other isoforms are known (19), though none of the mutations seem to be in positions known to influence protein behavior. Most cDNA constructs derived from the original sequence contain the innocuous mutation Q80R, probably resulting from a PCR error (11). Also, the gene has been resynthesized with altered codons and improved translational initiation sequences (see section on "Promoters, Codon Usage, and Splicing").

The chromophore is a *p*-hydroxybenzylideneimidazolinone (10, 20) formed from residues 65–67, which are Ser-Tyr-Gly in the native protein. Figure 2 shows the currently accepted mechanism (21–23) for chromophore formation. First, GFP folds into a nearly native conformation, then the imidazolinone is formed by nucleophilic attack of the amide of Gly67 on the carbonyl of residue 65, followed by dehydration. Finally, molecular oxygen dehydrogenates the  $\alpha$ - $\beta$  bond of residue 66 to put its aromatic group into conjugation with the imidazolinone. Only at this stage does the chromophore acquire visible absorbance and fluorescence. This mechanism is based on the following arguments: (a) Atmospheric oxygen is required for fluorescence to develop (21, 24). (b) Fluorescence of anaerobically preformed GFP develops with a simple exponential time course after air is readmitted (21, 25), which is essentially unaffected by the concentration of the GFP itself or of cellular cofactors. (c) Analogous imidazolinones autoxidize spontaneously (26). (d) The proposed

---

*Figure 1* GFP sequences. (Line 1) The wild-type (WT) *gfp10* gene as originally cloned and sequenced by Prasher et al (10). (Line 2) A popular humanized version (EGFP, Clontech Laboratories, Palo Alto, CA) (64) incorporating (a) an optimal sequence for translational initiation (66), including insertion of a new codon GTG; (b) mutation of Phe64 to Leu to improve folding at 37°C; (c) mutation of Ser65 to Thr to promote chromophore ionization; and (d) mutation of His231 to Leu, which was probably inadvertent and neutral. (Line 3) WT amino acid sequence. (Lines 4 and 5) Numbering of amino acids and differences between EGFP and WT. The inserted Val is numbered 1a to maintain correspondence with the WT numbering. Note that constructs derived from the natural *gfp10* cDNA contain an apparently neutral mutation Gln80 → Arg (Q80R) caused by a PCR error that changed the CAG codon to CGG (11). In some genes artificially resynthesized with different codons, this error was corrected (e.g. 63 and Clontech's EGFP) but was left as an arginine codon in other instances (40, 62).

ATG AGT AAA GGA GAA GAA CTT TTC ACT GGA GTT GTC CCA ATT CTT GTT GAA TTA GAT GGT 60  
 ATG GTG AGC AAG GGC GAG GAG CTG TTC ACC GGG GTG GTG CCC ATC CTG GTC GAG CTG GAC GGC  
 Met Ser Lys Gly Glu Glu Leu Phe Thr Gly Val Val Pro Ile Leu Val Glu Leu Asp Gly  
 1 Val 5 10 15 20  
 (1a)  
 GAT GTT AAT GGG CAC AAA TTT TCT GTC AGT GGA GAG GGT GAA GGT GAT GCA ACA TAC GGA 120  
 GAC GTA AAC GGC CAC AAG TTC AGC GTG TCC GGC GAG GGC GAG GGC GAT GCC ACC TAC GGC  
 Asp Val Asn Gly His Lys Phe Ser Val Ser Gly Glu Gly Glu Gly Asp Ala Thr Tyr Gly  
 25 30 35 40  
 AAA CTT ACC CTT AAA TTT ATT TGC ACT ACT GGA AAA CTA CCT GTT CCA TGG CCA ACA CTT 180  
 AAG CTG ACC CTG AAG TTC ATC TGC ACC ACC GGC AAG CTG CCC GTG CCC TGG CCC ACC CTC  
 Lys Leu Thr Leu Lys Phe Ile Cys Thr Thr Gly Lys Leu Pro Val Pro Trp Pro Thr Leu  
 45 50 55 60  
 GTC ACT ACT TTC TCT TAT GGT GTT CAA TGC TTT TCA AGA TAC CCA GAT CAT ATG AAA CAG 240  
 GTG ACC ACC CTG ACC TAC GGC GTG CAG TGC TTC AGC CGC TAC CCC GAC CAC ATG AAG CAG  
 Val Thr Thr Phe Ser Tyr Gly Val Gln Cys Phe Ser Arg Tyr Pro Asp His Met Lys Gln  
 Leu Thr 70 75 80  
 65  
 CAT GAC TTT TTC AAG AGT GCC ATG CCC GAA GGT TAT GTA CAG GAA AGA ACT ATA TTT TTC 300  
 CAC GAC TTC TTC AAG TCC GCC ATG CCC GAA GGC TAC GTC CAG GAC CGC ACC ATC TTC TTC  
 His Asp Phe Phe Lys Ser Ala Met Pro Glu Gly Tyr Val Gln Glu Arg Thr Ile Phe Phe  
 85 90 95 100  
 AAA GAT GAC GGG AAC TAC AAG ACA CGT GCT GAA GTC AAG TTT GAA GGT GAT ACC CTT GTT 360  
 AAG GAC GAC GGC AAC TAC AAG ACC CGC GCC GAG GTG AAG TTC GAG GGC GAC ACC CTG GTG  
 Lys Asp Asp Gly Asn Tyr Lys Thr Arg Ala Glu Val Lys Phe Glu Gly Asp Thr Leu Val  
 105 110 115 120  
 AAT AGA ATC GAG TTA AAA GGT ATT GAT TTT AAA GAA GAT GGA AAC ATT CTT GGA CAC AAA 420  
 AAC CGC ATC GAG CTG AAG GGC ATC GAC TTC AAG GAG GAC GGC AAC ATC CTG GGG CAC AAG  
 Asn Arg Ile Glu Leu Lys Gly Ile Asp Phe Lys Glu Asp Gly Asn Ile Leu Gly His Lys  
 125 130 135 140  
 TTG GAA TAC AAC TAT AAC TCA CAC AAT GTA TAC ATC ATG GCA GAC AAA CAA AAG AAT GGA 480  
 CTG GAG TAC AAC TAC AAC AGC CAC AAC GTC TAT ATC ATG GCC GAC AAG CAG AAG AAC GGC  
 Leu Glu Tyr Asn Tyr Asn Ser His Asn Val Tyr Ile Met Ala Asp Lys Gln Lys Asn Gly  
 145 150 155 160  
 ATC AAA GTT AAC TTC AAA ATT AGA CAC AAC ATT GAA GAT GGA AGC GTT CAA CTA GCA GAC 540  
 ATC AAG GTG AAC TTC AAG ATC CGC CAC AAC ATC GAG GAC GGC AGC GTG CAG CTC GCC GAC  
 Ile Lys Val Asn Phe Lys Ile Arg His Asn Ile Glu Asp Gly Ser Val Gln Leu Ala Asp  
 165 170 175 180  
 CAT TAT CAA CAA AAT ACT CCA ATT GGC GAT GGC CCT GTC CTT TTA CCA GAC AAC CAT TAC 600  
 CAC TAC CAG CAG AAC ACC CCC ATC GGC GAC GGC CCC GTG CTG CCC GAC AAC CAC TAC  
 His Tyr Gln Gln Asn Thr Pro Ile Gly Asp Gly Pro Val Leu Leu Pro Asp Asn His Tyr  
 185 190 195 200  
 CTG TCC ACA CAA TCT GCC CTT TCG AAA GAT CCC AAC GAA AAG AGA GAC CAC ATG GTC CTT 660  
 CTG AGC ACC CAG TCC GCC CTG AGC AAA GAC CCC AAC GAG AAG CGC GAT CAC ATG GTC CTG  
 Leu Ser Thr Gln Ser Ala Leu Ser Lys Asp Pro Asn Glu Lys Arg Asp His Met Val Leu  
 205 210 215 220  
 CTT GAG TTT GTA ACA GCT GCT GGG ATT ACA CAT GGC ATG GAT GAA CTA TAC AAA TAA TAA 720  
 CTG GAG TTC GTG ACC GCC GCC GGG ATC ACT CTC GGC ATG GAC GAG CTG TAC AAG TAA  
 Leu Glu Phe Val Thr Ala Ala Gly Ile Thr His Gly Met Asp Glu Leu Tyr Lys Stop  
 225 230 Leu 235

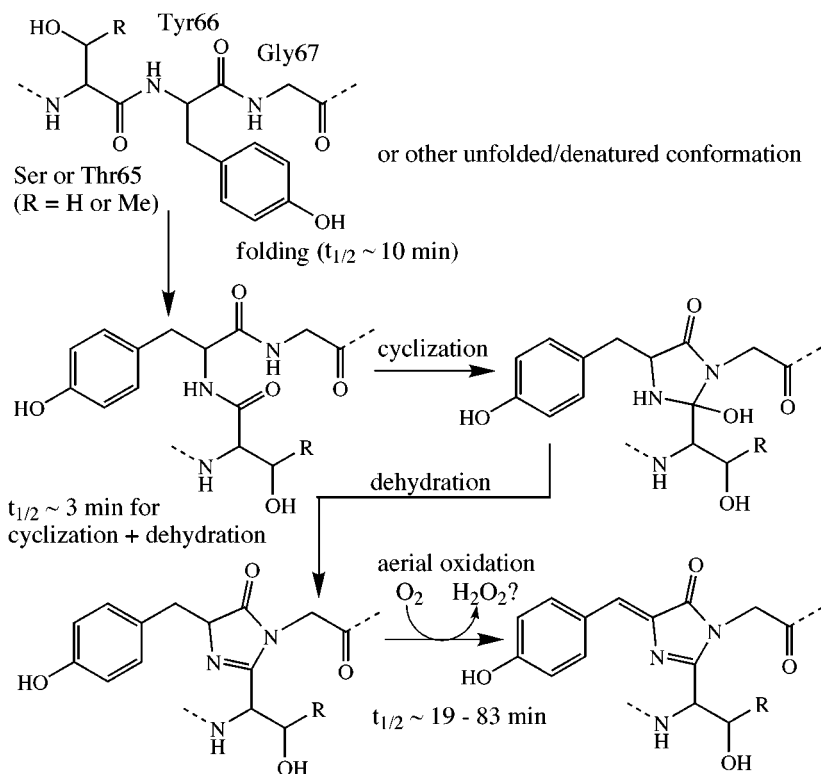


*Figure 2* Mechanism proposed by Cubitt et al (22) for the intramolecular biosynthesis of the GFP chromophore, with rate constants estimated for the Ser65  $\rightarrow$  Thr mutant by Reid & Flynn (23) and Heim et al (25).

cyclization is isosteric with the known tendency for Asn-Gly sequences to cyclize to imides (27). Glycine is by far the best nucleophile in such cyclizations because of its minimal steric hindrance, and Gly67 is conserved in all known mutants of GFP that retain fluorescence. (e) Electrospray mass spectra indicate that anaerobically preformed GFP loses only  $1 \pm 4$  Da upon exposure to air, consistent with the predicted loss of two hydrogens (22). This implies that the dehydration ( $-18$  Da) must already have occurred anaerobically and must precede oxidation. (f) Reid & Flynn (23) have extensively characterized the kinetics of *in vitro* refolding of GFP from bacterial inclusion bodies with no chromophore, urea-denatured protein with a mature chromophore, and denatured protein with a chromophore reduced by dithionite. Renaturation was measured by development of fluorescence and resistance to trypsin attack. Their

results support the sequential mechanism and provide the rate constants shown in Figure 2. However, many other aspects of the maturation mechanism remain obscure, such as the steric and catalytic roles of neighboring residues, the means by which mutations can improve folding efficiency, and the dependence of oxidation rate on the oxygen concentration and the protein sequence.

One predicted consequence of oxidation by  $O_2$  is that hydrogen peroxide,  $H_2O_2$ , is presumably released in 1:1 stoichiometry with mature GFP. This byproduct might explain occasions when high-level expression of GFP can be deleterious. Perhaps catalase could be useful in such cases. Some difficult GFPs seem to express most readily when targeted to peroxisomes and mitochondria (28; R Rizzuto, T Pozzan, personal communication). Is it a coincidence that these organelles are the best at coping with reactive oxygen species?

### *Crystal Structures; Tolerance of Truncations*

Although GFP was first crystallized in 1974 (4) and diffraction patterns reported in 1988 (29), the structure was first solved in 1996 independently by Ormö et al (30), Protein Data Bank accession number 1EMA, and by Yang et al (31), accession number 1GFL. Both groups relied primarily on multiple anomalous dispersion of selenomethionine groups to obtain phasing information from recombinant protein. Subsequent structures of other crystal forms and mutants (32–34a) have been solved by molecular replacement from the 1EMA coordinates. GFP is an 11-stranded  $\beta$ -barrel threaded by an  $\alpha$ -helix running up the axis of the cylinder (Figure 3). The chromophore is attached to the  $\alpha$ -helix and is buried almost perfectly in the center of the cylinder, which has been called a  $\beta$ -can (31, 34a). Almost all the primary sequence is used to build the  $\beta$ -barrel and axial helix, so that there are no obvious places where one could design large deletions and reduce the size of the protein by a significant fraction. Residues 1 and 230–238 were too disordered to be resolved; these regions correspond closely to the maximal known amino- and carboxyl-terminal deletions that still permit fluorescence to develop (35). A surprising number of polar groups and structured water molecules are buried adjacent to the chromophore (Figure 4). Particularly important are Gln69, Arg96, His148, Thr203, Ser205, and Glu222.

### *Dimerization*

The excitation spectrum of wild-type GFP changes its shape as a function of protein concentration, implying some form of aggregation (8). The spectroscopic effects of such aggregation are discussed in the section on “Absorbance and Fluorescence Properties.” In the Yang et al structure for wild-type GFP (31), the GFP is dimeric. The dimer interface includes hydrophobic residues Ala206, Leu221, and Phe 223 as well as hydrophilic contacts involving Tyr39, Glu142, Asn 144, Ser147, Asn149, Tyr151, Arg168, Asn170, Glu172, Tyr200,

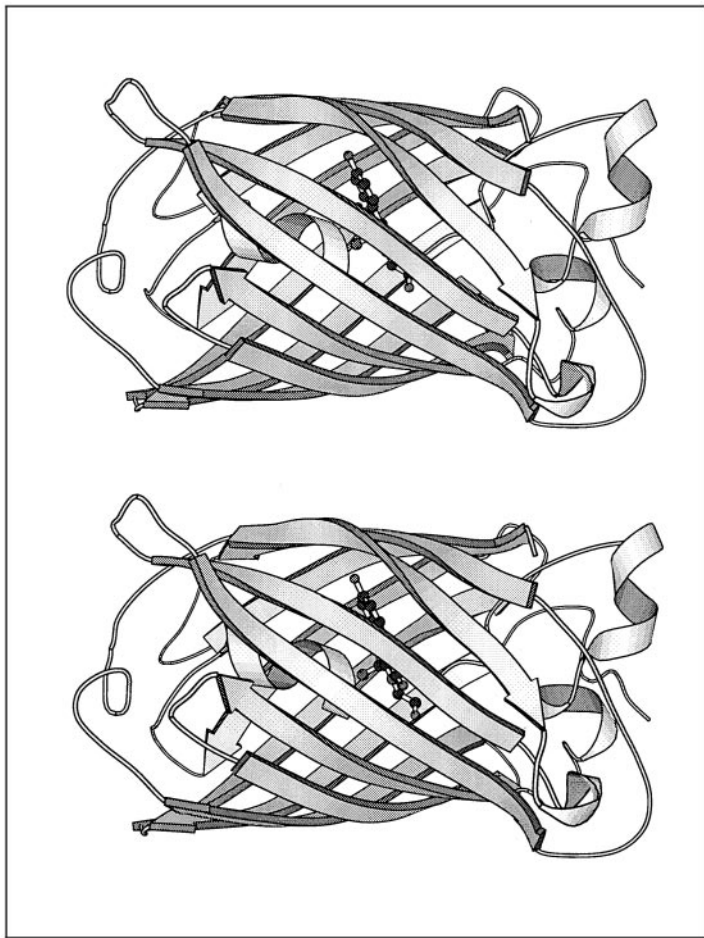


*Figure 3* Stereoview of the three-dimensional structure of GFP (30), showing 11  $\beta$ -strands forming a hollow cylinder through which is threaded a helix bearing the chromophore, shown in ball-and-stick representation. The drawing was prepared by the program MOLSCRIPT and is intended for viewing with uncrossed eyes. Figure courtesy of SJ Remington, University of Oregon.



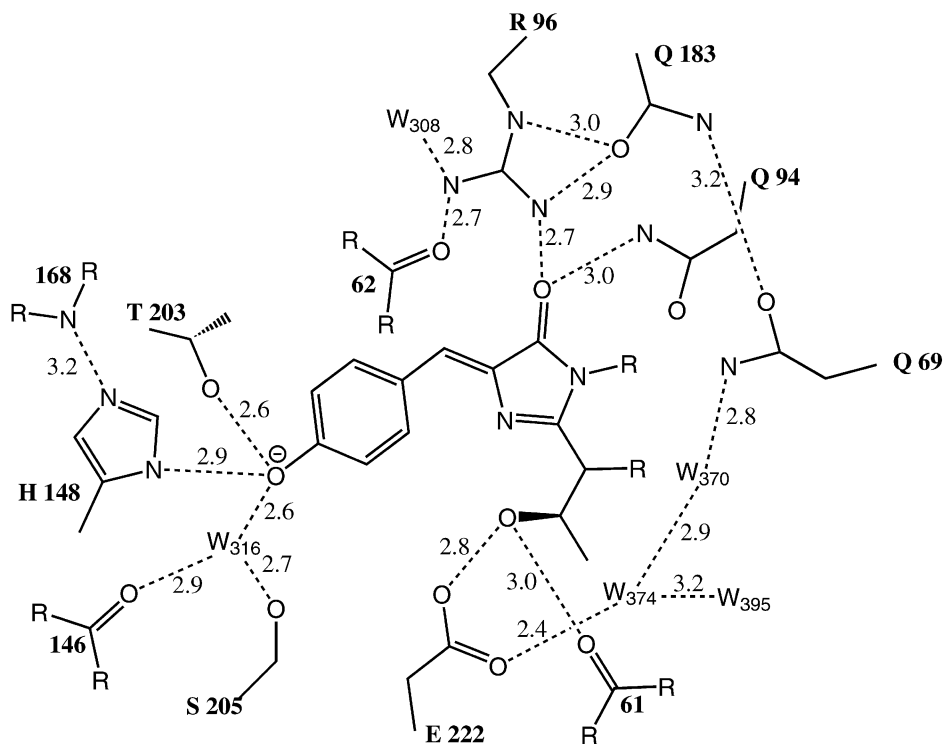


**Figure 4** Amino acid side chains, main chain carbonyls and amides, and solvent waters in the immediate vicinity of the chromophore of S65T GFP (30). Side chains are labeled with the one-letter code for the amino acid and the residue number. Main chain groups are labeled with the residue number. Water oxygens are denoted by W and the corresponding serial number within Protein Data Bank structure 1EMA. Probable hydrogen bonds are shown as dotted lines labeled with the distance between the heteroatoms in angstroms. Obviously the true three-dimensional relationships cannot be depicted accurately in this two-dimensional schematic. Figure courtesy of SJ Remington, University of Oregon.

Ser202, Gln204, and Ser208. However, the same wild-type GFP could also crystallize as a monomer (32), isomorphous to the monomeric crystals formed by the S65T mutant (30). Even though GFP can hardly be more concentrated than in a crystal, the formation of dimers seems to be highly dependent on crystal growth conditions rather than an obligatory feature of GFP (33). The dissociation constant for the homodimer has been estimated as 100  $\mu\text{M}$  (34a). By contrast, *Renilla* GFP is an obligate dimer, which is dissociated only under denaturing conditions (14).

## ABSORBANCE AND FLUORESCENCE PROPERTIES

*Classification of GFPs*

The currently known GFP variants may be divided into seven classes based on the distinctive component of their chromophores: class 1, wild-type mixture of neutral phenol and anionic phenolate; class 2, phenolate anion; class 3, neutral phenol; class 4, phenolate anion with stacked  $\pi$ -electron system; class 5, indole; class 6, imidazole; and class 7, phenyl. Each class has a distinct set of excitation and emission wavelengths (Table 1). Classes 1–4 are derived from polypeptides with Tyr at position 66, whereas classes 5–7 result from Trp, His, and Phe at that position. Structures of the resulting chromophores are shown in Figure 5, together with typical fluorescence spectra.

## WILD-TYPE MIXTURE OF NEUTRAL PHENOL AND ANIONIC PHENOLATE (CLASS 1)

The wild-type *Aequorea* protein has the most complex spectra of all the GFPs. It has a major excitation peak at 395 nm that is about three times higher in amplitude than a minor peak at 475 nm. In normal solution, excitation at 395 nm gives emission peaking at 508 nm, whereas excitation at 475 nm gives a maximum at 503 nm (21). The fact that the emission maximum depends on the excitation wavelength indicates that the population includes at least two chemically distinct species, which do not fully equilibrate within the lifetime of the excited state. At pH 10–11, when the protein is on the verge of unfolding, increasing pH increases the amplitude of the 475-nm absorbance or excitation peak at the expense of the 395-nm peak (8). The simplest interpretation is that the 475-nm peak arises from GFP molecules containing deprotonated or anionic chromophores, whereas the 395-nm peak represents GFPs containing protonated or neutral chromophores (21, 22). The latter would be expected to deprotonate in the excited state, because phenols almost always become much more acidic in their excited states. Light-induced ionization to the anion would explain why excitation of the neutral chromophores gives emission at greater than 500 nm, similar to but not quite identical to the direct excitation of anionic chromophores. Picosecond spectroscopy gives direct evidence for such excited-state proton transfer (36). After a flash at 395 nm, the emission shifts from a 460- to a 508-nm peak over about 10 ps. These kinetics can be slowed greatly by cooling to 77°K and increasing viscosity, or by deuterium substitution, which argue strongly for excited-state proton transfer.

During most light absorption/emission cycles, the proton transfer eventually reverses. However, occasionally the proton does not return to the chromophore, so the neutral chromophore is photoisomerized to the anionic form. Thus on

**Table 1** Spectral characteristics of the major classes of green fluorescent proteins (GFPs)

Mutation <sup>a</sup>	Common name	$\lambda_{\text{exc}}$ ( $\epsilon$ ) <sup>b</sup>	$\lambda_{\text{em}}$ (QY) <sup>c</sup>	Rel. fl. <sup>d</sup> @ 37°C	References <sup>e</sup>
<b>Class 1, wild-type</b>					
None or Q80R	Wild type	395–397 (25–30) 470–475 (9.5–14)	504 (0.79)	6	43, 45
F99S, M153T, V163A	Cycle 3	397 (30) 475 (6.5–8.5)	506 (0.79)	100	43, 45
<b>Class 2, phenolate anion</b>					
S65T		489 (52–58)	509–511 (0.64)	12	43–45
F64L, S65T	EGFP	488 (55–57)	507–509 (0.60)	20	43–45
F64L, S65T, V163A		488 (42)	511 (0.58)	54	44
S65T, S72A, N149K, M153T, I167T	Emerald	487 (57.5)	509 (0.68)	100	44
<b>Class 3, neutral phenol</b>					
S202F, T203I	H9	399 (20)	511 (0.60)	13	44
T203I, S72A, Y145F	H9–40	399 (29)	511 (0.64)	100	44
<b>Class 4, phenolate anion with stacked <math>\pi</math>-electron system (yellow fluorescent proteins)</b>					
S65G, S72A, T203F		512 (65.5)	522 (0.70)	6	44
S65G, S72A, T203H		508 (48.5)	518 (0.78)	12	44
S65G, V68L, Q69K S72A, T203Y	10C Q69K	516 (62)	529 (0.71)	50	44
S65G, V68L, S72A, T203Y	10C	514 (83.4)	527 (0.61)	58	44
S65G, S72A, K79R, T203Y	Topaz	514 (94.5)	527 (0.60)	100	44
<b>Class 5, indole in chromophore (cyan fluorescent proteins)</b>					
Y66W		436	485	—	21
Y66W, N146I, M153T, V163A	W7	434 (23.9) 452	476 (0.42) 505	61	44
F64L, S65T, Y66W, N146I, M153T, V163A	W1B or ECFP	434 (32.5) 452	476 (0.4) 505	80	44
S65A, Y66W, S72A, N146I, M153T, V163A	W1C	435 (21.2)	495 (0.39)	100	44
<b>Class 6, imidazole in chromophore (blue fluorescent proteins)</b>					
Y66H	BFP	384 (21)	448 (0.24)	18	44
Y66H, Y145F	P4–3	382 (22.3)	446 (0.3)	52	44
F64L, Y66H, Y145F	EBFP	380–383 (26.3–31)	440–447 (0.17–0.26)	100	43, 44
<b>Class 7, phenyl in chromophore</b>					
Y66F		360	442	—	22

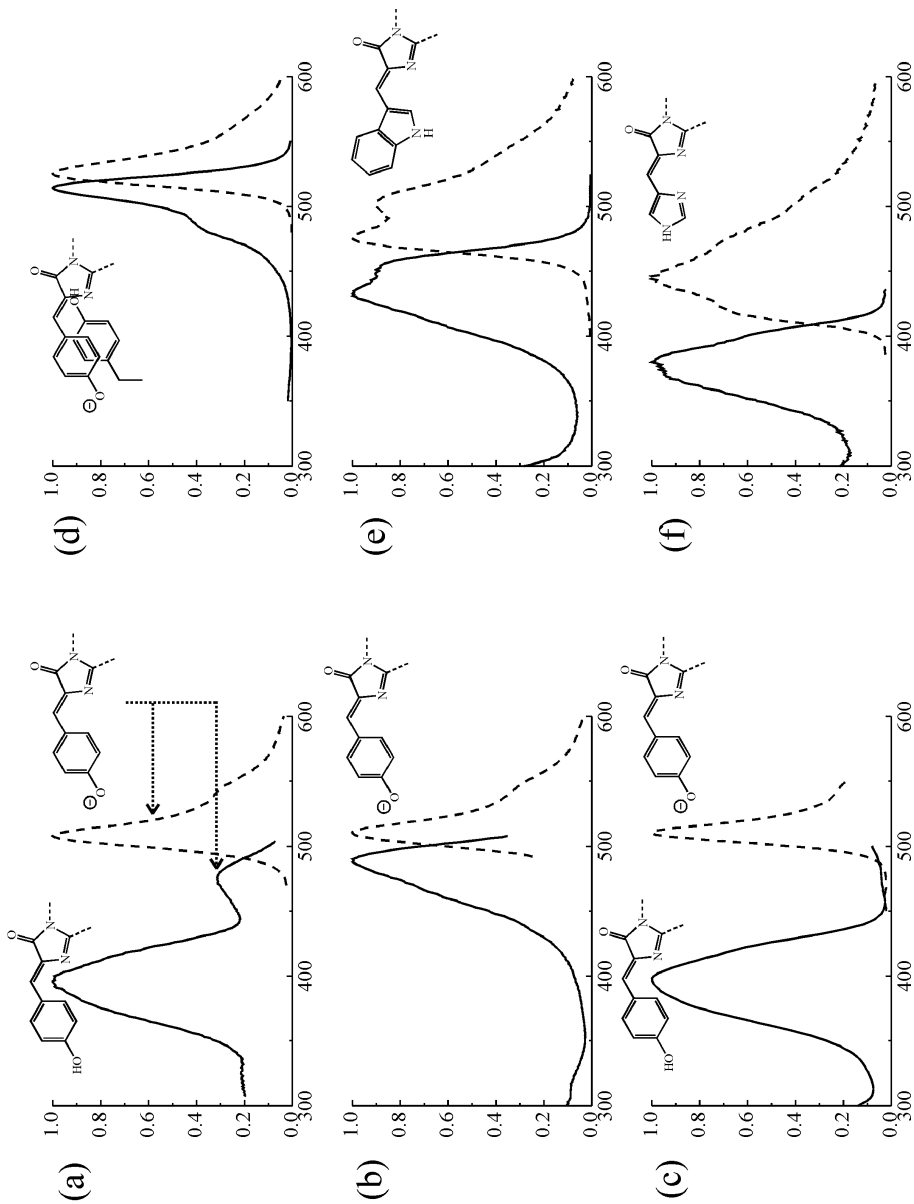
<sup>a</sup>Substitutions from the primary sequence of GFP (see Figure 1) are given as the single-letter code for the amino acid being replaced, its numerical position in the sequence, and the single-letter code for the replacement. Note that many valuable mutants have been left out of this table for reasons of brevity and because quantitative spectral and brightness data were not available; therefore omission does not imply denigration. Phenotypically neutral substitutions such as Q80R, H231L, and insertion of residue 1a (see Figure 1) have also been omitted.

<sup>b</sup> $\lambda_{\text{exc}}$  is the peak of the excitation spectrum in units of nanometers.  $\epsilon$  in parentheses is the absorbance extinction coefficient in units of  $10^3 \text{ M}^{-1} \text{ cm}^{-1}$ . Estimates of extinction coefficients have tended to increase as expression and purification are optimized; obsolete older values have been omitted. Two numbers separated by a dash indicate a range of estimates from different authors working under slightly different conditions. Two numbers on separate lines indicate two distinct peaks in the excitation spectrum.

<sup>c</sup> $\lambda_{\text{em}}$  is the peak of the emission spectrum in units of nanometers. QY in parentheses is the fluorescence quantum yield, which is dimensionless. The best figure of merit for the overall brightness of properly matured GFPs is the product of  $\epsilon$  and QY. See footnote b for explanation of pairs of values.

<sup>d</sup>Relative fluorescence intensities for proteins expressed in *Escherichia coli* at 37°C from the same vector background under similar conditions. These numbers include not only the intrinsic brightnesses measured by  $\epsilon \cdot \text{QY}$  but also the folding efficiencies at 37°C. They are only rough estimates, which will change under different expression conditions. They have been arbitrarily normalized to 100 for the brightest member of each class and cannot be used to compare different classes.

<sup>e</sup>References only for the quantitative spectral and brightness data. References to the origin and use of the mutants have been omitted for lack of space.



intense UV illumination, the 395-nm absorbance and excitation peak of the neutral form gradually declines and the 470-nm peak of the chromophore anion increases (22, 36, 37). Before illumination, wild-type GFP contains about a 6:1 ratio of neutral-to-anionic forms, but with enough UV the percentage of anionic form can increase several-fold. The probable mechanism (32, 33) is that proton transfer occurs via the hydrogen bonds of a buried water and Ser205 to Glu222. Meanwhile the side chain of Thr203 rotates to solvate and stabilize the phenolate oxyanion. In the crystal structure of monomeric wild-type GFP, Thr203 exists in two conformations: approximately 85% with the OH facing away from the phenol oxygen, and 15% with the OH rotated toward it (32). This proportion agrees well with the spectroscopic estimate for the ratio of neutral to anionic chromophores at equilibrium (36).

Wild-type GFP folds fairly efficiently when expressed at or below room temperature, but its folding efficiency declines steeply at higher temperatures. Presumably this natural temperature sensitivity is of no consequence to the jellyfish, which would never encounter warm water in the Pacific Northwest. Temperature sensitivity is restricted to the folding process. GFP that has matured properly at low temperature is stable and fluorescent at temperatures up to at least 65°C. The poor ability of GFP to mature in warm temperatures has been used in pulse-chase experiments in which the fate of fluorescent protein made at low temperatures is followed after restoration of normal warmth and simultaneous suppression of new fluorescence (38, 39). However, for other applications it would be desirable to have a GFP that works well at 37°C.

The most extensive attempt to develop such a mutant while preserving the complex wild-type spectrum utilized DNA shuffling (40), a technique for recombining various mutations while creating new ones. This approach produced a triple mutant, F99S, M153T, V163A, which improved 37°C-folding, reduced aggregation at high concentrations, and increased the diffusibility of the protein inside cells (37). The latter two mutations had already been found by more conventional mutagenesis procedures (41, 42). Such folding mutations do not

←

*Figure 5* Fluorescence excitation and emission spectra (solid and dashed lines, respectively) for typical members of the six major classes of GFP mutants, together with the chromophore structures believed to be responsible for the spectra. Spectra have been normalized to a maximum amplitude of 1. For comparison of absolute brightnesses, see the extinction coefficients and quantum yields in Table 1. When only one structure is drawn, both excitation and emission spectra arise from the same state of chromophore protonation. The actual GFPs depicted are (a) wild-type, (b) Emerald, (c) H9-40, (d) Topaz, (e) W1B, and (f) P4-3. The detailed substitutions within each of these variants are listed in Table 1.

increase the intrinsic brightness of properly matured GFP molecules. Such brightness is measured by the product of extinction coefficient and fluorescence quantum yield (Table 1). The folding mutations merely increase the percentage of molecules that mature properly under adverse conditions, such as 37°C and high GFP concentrations that promote aggregation (33, 43–45). Although the folding mutations are highly valuable and should be incorporated routinely into new constructs, they produce less dramatic or no improvements at lower temperatures and levels of expression. Also the increments in brightness achieved by compounding such mutations will be limited by the obvious fact that folding cannot exceed 100% efficiency.

The coexistence of neutral and anion chromophores giving two excitation peaks in the wild-type spectrum has a few advantages and many disadvantages for cell biological applications. If the GFP fluorescence is to be detected by the naked eye, UV excitation is convenient (40) because UV is inherently invisible. However, because intense UV can damage the eye, an external excitation-blocking filter would be advisable even for visual inspection. Also, scattering, autofluorescence, and the possibility of tissue damage are more severe with UV excitation. Excitation at the 470-nm peak would reduce these problems but is inefficient because only 15% of the protein has the anionic chromophore that absorbs there. The photoisomerization is a major hindrance to quantitation of images, but it also permits the diffusion or trafficking of GFP-labeled proteins to be monitored by locally irradiating a cell with a point or stripe of intense UV and then imaging the subsequent fate of the photoisomerized protein with 470-nm excitation (37).

**PHENOLATE ANION IN CHROMOPHORE (CLASS 2)** GFPs with phenolate anions in the chromophore have become the most widely used class for routine cell biological use because they were the first group to combine high brightness with simple excitation and emission spectra peaking at wavelengths very similar to fluorescein, the most popular small-molecule fluorophore. The most commonly used mutation to cause ionization of the phenol of the chromophore is a replacement of Ser65 by Thr, or S65T (25), though several other aliphatic residues such as Gly, Ala, Cys, and Leu have roughly similar effects (25, 46, 47). The triple mutation F64M, S65G, Q69L, found by random mutagenesis around the chromophore, has achieved considerable popularity under the name RSGFP4 (46). In both S65T and RSGFP4, the wild-type 395-nm excitation peak due to the neutral phenol is suppressed, and the 470- to 475-nm peak due to the anion is enhanced five- to sixfold in amplitude and shifted to 489–490 nm (25, 46, 48). The oxidation to the mature fluorophore was about fourfold faster in S65T than in the wild type (25). Like wild-type GFP, S65T folds fairly efficiently

when expressed at room temperature or below but tends to misfold and produce mostly nonfluorescent aggregates at higher temperatures. Because of the obvious interest in expression at 37°C, much effort has been devoted to finding additional mutations that give greater brightness at warmer temperatures. The most often used of these have been F64L (47) and V163A (42), though other mutations such as S72A, N149K, M153T, and I167T (33) (Table 1) can also be helpful alone or in combination. As with GFPs of wild-type spectra, such mutations improve only folding efficiency, not the brightness of properly folded molecules.

The probable mechanism by which replacement of Ser65 promotes chromophore ionization (30, 32) is that only Ser65 can donate a hydrogen bond to the buried side chain of Glu222 to allow ionization of that carboxylate, which is within 3.7 Å of the chromophore. Gly, Ala, and Leu cannot donate hydrogen bonds, and Thr and Cys are too large to adopt the correct conformation in the crowded interior of the protein. Such residues at position 65 force the carboxyl of Glu222 to remain neutral. The other polar groups solvating the chromophore are then sufficient to promote its ionization to an anion, whereas if Glu222 is an anion, electrostatic repulsion forbids the chromophore from becoming an anion as well. This hypothesis explains why mutation of Glu222 to Gly gives the same spectral shape and wavelengths (49) as Ser65 mutations. However, practical applications of E222G have not been reported.

NEUTRAL PHENOL IN CHROMOPHORE (CLASS 3) Ionization of the chromophore cannot only be favored but be repressed. Mutation of Thr203 to Ile (21, 49) largely suppresses the 475-nm excitation peak, leaving only the shorter wavelength peak at 399 nm. Presumably a chromophore anion cannot be adequately solvated once the OH of Thr203 is gone, so the chromophore is neutral in almost all the ground-state molecules. However, the emission is still at 511 nm because the excited state remains acidic enough to eject a proton. This mutant and its folding-optimized descendants (Table 1) could be valuable alternatives for UV-excited green fluorescence without the complicated photochemistry of wild-type (class 1) GFPs. Because they lack an excitation maximum near 479–490 nm, they could be used in conjunction with the phenolate anion (class 2) GFPs for double-labeling. Images taken with the two different excitation bands near 400 and 480 nm but the same greater-than-500-nm emission would be compared. Even though the spectral contrast between the two GFPs would not be as great as when both excitation and emission wavelengths are varied, the use of two excitation wavelengths fits the many imaging systems designed for excitation-ratioing indicators and avoids any image registration problems created by alternating emission filters. The neutral phenol GFPs also

have the largest gap in wavelengths between excitation and emission peaks of any of the GFPs. This large Stokes' shift could be advantageous in supporting laser action, where it is important that the dye should have as little absorbance as possible at the wavelengths of fluorescence and lasing.

PHENOLATE ANION WITH STACKED  $\pi$ -ELECTRON SYSTEM (CLASS 4) The longest wavelengths currently available by mutation result from stacking an aromatic ring next to the phenolate anion of the chromophore. So far the aromatic ring has always come from the side chain of residue 203, and residue 65 is Gly or Thr instead of Ser, to promote ionization of the chromophore. All four aromatic residues at that position 203 (His, Trp, Phe, and Tyr) increase the excitation and emission wavelengths by up to 20 nm, with the shifts increasing in the stated order (30). These mutants were rationally designed from the crystal structure of S65T GFP in the expectation that the additional polarizability around the chromophore and  $\pi$ - $\pi$  interaction would reduce the excited state energy, that is, increase both the excitation and emission wavelengths. The mutants would have been nearly impossible to find by random mutagenesis, because all three bases in the original codon (ACA) encoding Thr203 would have to be replaced to encode an aromatic amino acid, and any random mutation rate high enough to give a significant probability of changing three bases in one codon would mutate so many other residues as to kill the protein.

The actual crystal structure of a mutant containing Tyr203 has verified that its aromatic ring stacks next to the chromophore (RM Wachter, GT Hanson, AB Cubitt, K Kallio, RY Tsien, SJ Remington, manuscript in preparation). Mutation of Gln69 to Lys (Q69K) gives an additional shift of about 1–2 nm, resulting in an emission peak around 529 nm, the longest now known (Table 1). Although 529 nm itself is rather greenish, the tail at longer wavelengths is sufficient to give the fluorescence an overall yellowish appearance, which is clearly distinguishable by eye from the more greenish emission of GFP classes 1–3. Therefore class 4 GFPs have been called YFPs for yellowish fluorescent proteins (50), though this name has also been used for a fluorescent protein from *Vibrio fischeri* (16). The so-called BioYellow variety marketed by Pharmingen (51) is identical to RSGFP4 (46), a class 2 GFP with emission maximum at 505 nm, the same as the wild type.

INDOLE IN CHROMOPHORE DERIVED FROM Y66W (CLASS 5) Substitution of Trp for Tyr66 produces a new chromophore with an indole instead of a phenol or phenolate (21). Excitation and emission wavelengths are 436 and 476 nm, intermediate between neutral phenol and anionic phenolate chromophores. The increased bulk of the indole requires many additional mutations to restore



reasonable brightness (41), but when such mutations are provided, the overall performance is fairly good (Table 1). These proteins are called cyan fluorescent proteins, or CFPs, because of their blue-green or cyan emission. One curious and so far unexplained feature (Figure 5) is that most have double-humped rather than conventional single excitation and emission peaks. The origin of the doubled emission peaks must be vibrational levels or other quantum states that equilibrate within the lifetime of the excited state, because their shapes and relative amplitudes are the same regardless of the excitation wavelength.

IMIDAZOLE IN CHROMOPHORE DERIVED FROM Y66H (CLASS 6) Substitution of His for Tyr 66 puts an imidazole in the chromophore (21) and shifts the wavelengths yet shorter than Trp66. The excitation and emission peaks are around 383 and 447 nm (Table 1), so the emission is blue. A convenient abbreviation is therefore BFP, although other blue fluorescent proteins [e.g. spent aequorin and lumazine-containing proteins from *Photobacterium phosphoreum* (15)] have previously shared the same acronym. Crystal structures for several BFPs have been solved (33, 34). As usual, these proteins benefit considerably from folding mutations (33, 41). BFP and a UV-excitable GFP permit double-labeling of cellular structures with two emission colors arising from a common excitation wavelength near 390 nm (28). However, even with folding improvements BFP still suffers from a relatively low fluorescence quantum yield and relatively easy bleaching (28). A functional dye laser has been constructed with purified BFP as the gain medium, but the duration of lasing at 450 nm is limited by protein bleaching (SJ Remington, D Alavi, M Raymer, RY Tsien, manuscript in preparation).

PHENYL IN CHROMOPHORE DERIVED FROM Y66F (CLASS 7) The very shortest wavelengths are obtained with Phe at 66 (22). This mutant has been little investigated because no obvious practical use for proteins requiring such short wavelength excitation has been proposed. Nevertheless it proves that any aromatic residue at position 66 can form a chromophore.

### *General Relation of Structure to Spectra*

The denatured wild-type protein absorbs maximally at 384 nm at neutral or acidic pH and at 448 nm at alkaline pH, with a  $pK_a$  of 8.1 (7). This rough similarity to the absorbance and excitation maxima of the intact protein was a primary motivation for assigning the 395- and 470-nm excitation peaks of the latter to the neutral and anionic chromophores. Denatured GFPs or small proteolytic fragments carrying the chromophore are essentially totally nonfluorescent, presumably because the chromophore is unprotected from quenching by jostling water dipoles, paramagnetic oxygen molecules, or *cis-trans*

isomerization (7, 52). The slight difference in absorbance wavelengths between denatured and intact proteins is not unreasonable for the structured environment of the latter. In particular, Arg96 puts a positively charged guanidinium quite close to the carbonyl group of the imidazolinone. This cation would electrostatically stabilize increased electron-density on the carbonyl oxygen in the chromophore's excited state. This electrostatic attraction would explain much of the red shift of intact protein relative to denatured protein. Indeed, mutation of Arg96 to Cys in S65T blue-shifts the excitation maximum from 489 to 472 nm and the emission maximum from 511 to 503 nm (R Ranganathan, personal communication), supporting a major role for Arg96 in lowering the energy of the excited state. Theoretical calculations of the energy levels of the chromophore in vacuo have led to the proposal that the imidazolinone-ring nitrogen adjacent to the hydroxybenzylidene must be protonated (53). However, the large effects on the chromophore of buried water molecules and the microenvironment supplied by the protein (52) would seem to provide a chemically more plausible explanation.

### *Two-Photon Excitation*

One of the most promising new techniques in high-resolution fluorescence microscopy is two-photon excitation (54), in which two infrared photons hit a fluorophore within a few femtoseconds of each other and sum their energy to simulate a single photon of half the wavelength, that is, ultraviolet to blue. Such coincidence of infrared photons requires extremely high fluxes and therefore occurs to a significant extent only at the focus of a microscope objective of high numerical aperture, illuminated by a pulsed laser. Because other regions of the specimen are effectively not excited, they neither emit fluorescence nor are subject to photobleaching or photodynamic damage. As in confocal microscopy, the image is built up by scanning the focus point in a raster, but unlike confocal microscopy, out-of-focus planes are protected from bleaching, which is a tremendous advantage for two-photon excitation.

GFPs are quite good fluorophores for two-photon excitation. Wild-type GFP is readily excited with 780- to 800-nm pulses (43, 54–56), which are in the optimal output range for commercial mode-locked titanium-sapphire lasers. However, the photoisomerization proceeds just as with 390- to 400-nm single-photon excitation (55). Class 3 (neutral phenol) GFP mutants have not been tried but should be better because they disfavor photoisomerization. S65T, the prototypic class 2 GFP mutant, is optimally excited near 910 nm and has a slightly higher two-photon cross-section than the wild type (54). Two-photon excitation is also effective on class 6 (imidazole) blue mutants (43) as well as class 5 (indole) cyan mutants (H Fujisaki, G Fan, A Miyawaki, RY Tsien, unpublished observations).

### *Effects of pH*

As noted above, wild-type GFP at high pH (11–12) loses absorbance and excitation amplitude at 395 nm and gains amplitude at 470 nm (8, 57). Such pH values, though mechanistically revealing, are almost never encountered in biology. Wild-type GFP is also quenched by acidic pH values with an apparent  $pK_a$  near 4.5. Several of the mutants with enhanced spectral properties at pH 7 are actually more acid sensitive than is the wild type; thus EGFP is 50% quenched at pH 5.5 (43).  $pK_a$ s as high as 6.8 are found in some of the class 4 mutants with Thr203 replaced by an aromatic residue (J Llopis, RY Tsien, manuscript in preparation; R Wachter, SJ Remington, personal communication). The mechanistic explanation for these relatively high  $pK_a$ s is not entirely clear. Loss of the Thr203 hydroxyl would indeed be expected to destabilize the phenolate form of the chromophore. However, the effect of acid is to quench the fluorescence altogether rather than simply shift it toward the short wavelengths expected of a protonated chromophore. The sensitivity of some GFPs to mildly acidic pH values carries both advantages and disadvantages. Such GFPs could be quenched to a major extent in acidic organelles such as lysosomes, endosomes, and Golgi compartments. The pH sensitivity of some GFPs can also be put to good use to measure organellar pH (J Llopis, RY Tsien, manuscript in preparation; R Wachter, SJ Remington, personal communication) by targeting appropriate GFPs to those locations.

### *Effects of Temperature and Protein Concentrations*

Higher GFP concentrations amplify the main excitation peak at 395 nm at the expense of the subsidiary peak at 470 nm (8). Because the 395- and 470-nm peaks are believed to result from neutral and anionic fluorophores, respectively, aggregation probably inhibits ionization of the fluorophores. Increasing temperature from 15 to 65°C modestly decreases the 395-nm and increases the 470-nm excitation peak of mature wild-type GFP. Yet higher temperatures cause denaturation, with 50% of fluorescence lost at 78°C (8). As already mentioned, much more modest temperature increases from 20 to 37°C can profoundly decrease maturation efficiency of GFPs lacking mutations to improve folding.

### *Effects of Prior Illumination*

GFPs have a variety of remarkable abilities to undergo photochemical transformations, which enables visualization of the diffusion or trafficking of GFP-tagged proteins. A defined zone within a cell or tissue is momentarily exposed to very bright illumination, which initiates the photochemistry. The subsequent fate of the photoconverted protein is imaged over time. At least four distinct types of semipermanent photochemical transformation have been reported from one or more GFPs: (a) simple irreversible photobleaching, (b) conversion from

a 395- to 475-nm excitation maximum, (c) loss of 488-nm-excited fluorescence, reversible by illumination at 406 nm, and (d) generation of rhodamine-like orange or red fluorescence upon illumination at 488 nm under strictly anaerobic conditions (58).

**IRREVERSIBLE PHOTBLEACHING** Photobleaching is the simplest and most universal behavior of fluorophores. Most GFPs are relatively resistant to photobleaching (22, 59), perhaps because the fluorophore is well shielded from chemical reactants such as O<sub>2</sub>. The bleach rate of the prototypic class 2 GFP, the S65T mutant, was reported to be relatively indifferent to equilibration with 0–100% oxygen or addition of quenchers of triplet states, singlet oxygen, and radicals (59). Nevertheless, with sufficient laser power, photobleaching is easily observed and exploited for measurements of fluorescence recovery (37, 59, 60). The class 6 mutants (BFPs) are generally more photosensitive than classes 1–5 (28). Cell-permeant antioxidants may be helpful in protecting such GFPs from bleaching. An example is Trolox, 6-hydroxy-2,5,7,8-tetramethylchroman-2-carboxylic acid, a water-soluble vitamin E analog commercially available from Aldrich Chemical Co., Milwaukee, WI.

**SHIFTING TO A LONGER-WAVELENGTH EXCITATION PEAK** This behavior is characteristic of wild-type and other class 1 GFPs (11, 22, 36). As discussed previously, the mechanism is probably a light-driven proton transfer from the neutral chromophore to the carboxylate of Glu222, yielding an anionic chromophore and a protonated Glu222 (32). This UV-induced enhancement of the blue excitation peak has been exploited to measure lateral diffusion of GFP-tagged proteins (37). Because the proton transfer is mediated by Thr203 and Ser205, mutation of those residues might be a promising way to enhance this photochromic effect. Indeed, UV irradiation of the double mutant T203S, S205T increases the amplitude of its long-wavelength excitation peak 11.8-fold, whereas wild-type GFP under the same conditions increases by at most 3.6-fold (R Heim, RY Tsien, unpublished information).

**REVERSIBLE LOSS OF LONGER-WAVELENGTH EXCITATION PEAK; SINGLE MOLECULE DETECTION** The opposite behavior, a shift from a longer to a shorter excitation wavelength, seems to occur in class 4 mutants. Upon intense laser illumination and observation of the fluorescence from single molecules immobilized in a polyacrylamide gel, such mutants both blink reversibly on a time scale of seconds and switch the fluorescence off over tens of seconds (61). However, the apparent bleaching can be reversed by illumination at short wavelengths such as 406 nm. Probably the chromophore, which is normally mostly anionic, can eventually be driven into a protonated state with an excitation maximum near 405 nm, whereupon it appears nonfluorescent and bleached to the probe

laser at 488 nm. However, excitation of the protonated state then restores the normal anionic state. Such cycling can be repeated many times with apparently no fatigue, so that it potentially represents a basis for an optical memory at the single molecule level. It might also be particularly advantageous for multiple determinations of diffusion or trafficking on the same region of interest.

**ANAEROBIC PHOTOCONVERSION TO A RED FLUORESCENT SPECIES** A variety of GFPs, including wild-type, S65T, and EGFP, undergo a remarkable photoconversion to a red fluorescent species under rigorously anaerobic conditions, for example, in microorganisms that have exhausted the oxygen in the medium, or in the presence of oxygen scavengers such as glucose plus glucose oxidase and catalase (58). The nature of this species emitting at 600 nm remains to be clarified. This effect has been used to measure the diffusibility of GFP in live bacteria. One complication is that the red emission develops with an exponential time constant of about 0.7 s after the illuminating flash (58).

## EXPRESSION, FORMATION, MATURATION, RENATURATION, AND OBSERVATION

### *Promoters, Codon Usage, and Splicing*

The expression level and detectability of GFP depend on many factors, the most important of which are summarized in Table 2. Obviously the more copies of the gene and the stronger the promoters/enhancers driving its transcription, the more protein that will be made per cell. In plants, it has been important to alter the original codon usage to eliminate a cryptic splice site (62). Codons have also been altered to conform to those preferred in mammalian systems (63, 64) and in the pathogenic yeast *Candida albicans* (65). Some authors have found such codon alterations to improve expression levels in mammalian systems (44, 63, 64), whereas others have found little improvement (43). Because the mammalianized genes are now widely available and may well be beneficial, they might as well be incorporated into all new GFP constructs for use in vertebrates. Our impression is that mammalian codons do not hurt expression levels in bacteria. Yet another improvement for mammalian systems is the inclusion of an optimal ribosome-binding site, also known as a Kozak sequence for translational initiation (66). Such a sequence requires insertion of an additional codon immediately after the starting methionine, as shown in Figure 1. The additional valine or alanine (40) does not seem to interfere with protein function; we prefer to number it 1a so that the numbering of the subsequent amino acids continues to correspond with the wild-type numbering. GFP can be expressed with reasonable efficiency in a cell-free in vitro translation system (67), a finding that confirms the protein can fold autonomously.

**Table 2** Factors affecting the detectability of green fluorescent protein (GFP)

---



---

Total amount of GFP (picked out by antibodies, or by position on gel if GFP is abundant enough)
Number of copies of gene, duration of expression
Strength of transcriptional promoters and enhancers
Efficiency of translation including Kozak sequence and codon usage
Absence of mRNA splicing, protein degradation and export
Efficiency of posttranslational fluorophore formation
Solubility vs. formation of inclusion bodies
Availability of chaperones
Hindrance to folding because of unfortunate fusions to host proteins
Time, temperature, availability of O <sub>2</sub> , and intrinsic rate of cyclization/oxidation
Molecular properties of mature GFP
Wavelengths of excitation and emission
Extinction coefficient and fluorescence quantum yield
Susceptibility to photoisomerization/bleaching
Dimerization
Competition with noise and background signals
Autofluorescence of cells or culture media at preferred wavelengths
Location of GFP, diffuse vs. confined to small subregions of cells or tissues
Quality of excitation and emission filters and dichroic mirrors
Sensitivity, noise, and dark current of photodetector

---

### *Folding Mutations and Thermotolerance*

As mentioned previously, several mutations improve the ability of GFP to fold at temperatures above those to which the jellyfish would have been exposed. Most of them replace bulky residues with smaller ones. Their scattered locations throughout the three-dimensional structure of the mature protein (Figure 6) give little hint as to why they should help folding and maturation. Of course, the X-ray structures are all determined on well-folded mature proteins. At the stage when the mutations are needed, the protein is presumably less well ordered. As an alternative to mutating the GFP, the presence of chaperones can also help GFP fold (68). Aside from the potential technical importance of providing chaperones, this finding makes GFP a useful substrate for testing chaperone function (69), since GFP provides a continuous nondestructive assay for successful folding.

### *Requirement for O<sub>2</sub>*

The requirement for O<sub>2</sub> to dehydrogenate the  $\alpha,\beta$  bond of residue 66 (21, 23, 24) means that GFP probably cannot become fluorescent in obligate anaerobes. So far this is the only fundamental limitation on the range of systems in which GFP can be expressed. Once GFP is matured, O<sub>2</sub> has no further effect (59). The oxidation seems to be the slowest step (Figure 2) in the maturation of GFP (23),

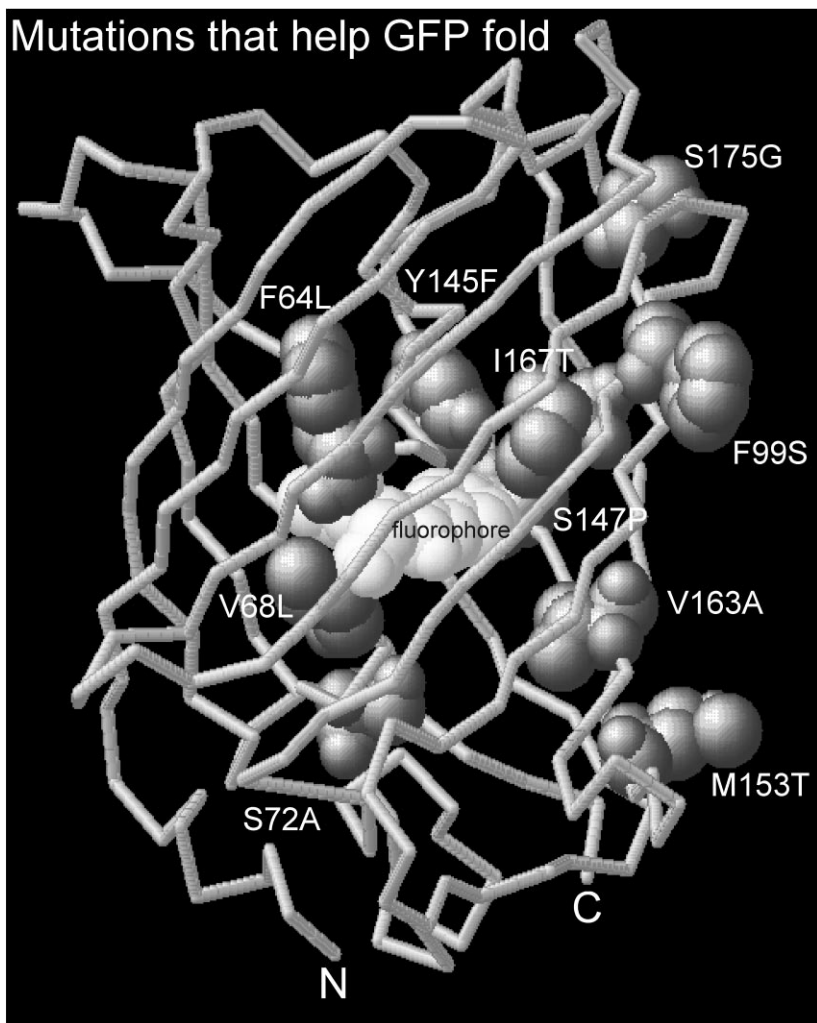


*Figure 6* Location on the GFP crystal structure (30) of the most important sites that improve folding at 37°C. The amino acids shown in space-filling representation are the wild-type residues that are replaced by the mutations listed.

so it imposes the ultimate limit on the ability of GFP fluorescence to monitor rapid changes in gene expression. Considering its importance, surprisingly little work has been done on how to accelerate this oxidation. The dependence of rate on oxygen pressure has not been characterized, so it is unknown whether  $pO_2$  higher than ordinary atmospheric would speed up the reaction. The mutant S65T has been reported to oxidize with an exponential time constant of 0.5 h, 4 times faster than the 2 h for wild-type protein under parallel conditions (25). Strong reductants such as dithionite can decolorize mature GFP (24, 52), probably by rehydrogenating the chromophore. Such reduction may also require that the GFP become denatured to allow access to the buried chromophore (23).

### *Histology in Fixed Tissues*

Although the prime advantage of GFP is its ability to generate fluorescence in live tissue, its fluorescence does survive glutaraldehyde and formaldehyde fixatives (11). Occasional problems in maintaining fluorescence during fixation may result from uncontrolled acidity of the fixative solution or the use of excessive organic solvents, which denature the protein and destroy the fluorescence (7).

## PASSIVE APPLICATIONS OF GFP

Cell biological applications of GFP may be divided into uses as a tag or as an indicator. In tagging applications, the great majority to date, GFP fluorescence merely reflects levels of gene expression or subcellular localizations caused by targeting domains or host proteins to which GFP is fused. As an indicator, GFP fluorescence can also be modulated posttranslationally by its chemical environment and protein-protein interactions.

### *Reporter Gene, Cell Marker*

The first proposed application of GFP was to detect gene expression in vivo (11), especially in the nematode *Caenorhabditis elegans*, whose cuticle hinders access of the substrates required for detecting other reporter genes. GFP was particularly successful at confirming the pattern of expression of the *mec-7* promoter, which drives the formation of  $\beta$ -tubulin in a limited number of mechanosensory neurons. GFP's independence from enzymatic substrates is likewise particularly promising in intact transgenic embryos and animals (70–76) and for monitoring the effectiveness of gene transfer (48, 77, 78). However, GFP seems to need rather strong promoters to drive sufficient expression for detection, especially in mammalian cells. Most published examples, even those using brightened GFPs with mutations to promote folding at 37°C, have used constitutive promoters from viruses such as cytomegalovirus (CMV), SV40,



or HIV long terminal repeat (79), or strong exogenous regulators such as the tetracycline transactivator system (80, 81), rather than native genetic response elements modulated by endogenous signals.

The somewhat disappointing sensitivity of GFP as a so-called gene-tag is probably an inherent result of its lack of amplification. GFP is not an enzyme that catalytically processes an indefinite number of substrate molecules. Instead, each GFP molecule produces at most one fluorophore. It has been estimated that 1  $\mu\text{M}$  well-folded wild-type GFP molecules are required to equal the endogenous autofluorescence of a typical mammalian cell (55), that is, to double the fluorescence over background. Mutant GFPs with improved extinction coefficients might improve this detection limit six- to tenfold (43) (see also Table 1), but 0.1  $\mu\text{M}$  GFP is still approximately  $10^5$  copies per typical cell of 1–2 pL volume. This estimate already assumes perfect GFP maturation; imperfect or incomplete maturation would raise the threshold copy number even further. The ultimate sensitivity limit is set not by instrumentation but by cellular autofluorescence.

If cytosolic GFP is inadequately sensitive as a reporter gene, two alternatives should be considered. If the gene product can be detected by microscopic imaging with subcellular resolution, then targeting the GFP to a defined sub-compartment of the cell can greatly reduce the number of molecules required. The GFP becomes highly concentrated, and the surrounding unlabeled region of the cell provides an internal reference for the autofluorescence background, which is usually diffuse in each cell. It is far easier to see local contrast within a cell than to quantitate a cell's average fluorescence relative to unlabeled standards. Thus as few as 300–3000 GFPs packed into a centrosome are readily visible as a green dot inside a cell (82). However, compartmentation of the GFP does not help with nonimaging detection methods such as fluorometry in cuvettes or microtiter plates or fluorescence-activated cell sorting (FACS). A different solution is to use reporter gene products that can enzymatically catalyze a large change in the fluorescence of substrates that can be loaded into intact, fully viable cells. For example, the bacterial enzyme  $\beta$ -lactamase can be detected at levels as low as 60 pM in single mammalian cells (50 molecules per cell) with substrates loaded as membrane-permeant esters (83).

### *Fusion Tag*

The most successful and numerous class of GFP applications has been as a genetic fusion partner to host proteins to monitor their localization and fate. The gene encoding a GFP is fused in frame with the gene encoding the endogenous protein and the resulting chimera expressed in the cell or organism of interest. The ideal result is a fusion protein that maintains the normal functions and localizations of the host protein but is now fluorescent. The range of successful

fusions is now much greater than previously tabulated (22). Not all fusions are successful, but the failures are almost never published, so it is difficult to assess the overall success rate. GFP has been targeted successfully to practically every major organelle of the cell, including plasma membrane (37, 84–87), nucleus (28, 38, 87–92), endoplasmic reticulum (50, 60, 93), Golgi apparatus (93), secretory vesicles (39, 94), mitochondria (28, 89, 95, 96), peroxisomes (97), vacuoles (98), and phagosomes (99). Thus the size and shape of GFP and the differing pHs and redox potentials of such organelles do not seem to impose any serious barrier. Even specific chromosomal loci can be tagged indirectly by inserting multiple copies of Lac operator sites and decorating them with a fusion of GFP with the Lac repressor protein (100). In general, fusions can be attempted at either the amino or carboxyl terminus of the host protein, sometimes with intervening spacer peptides. However, the crystal structures of GFP (30, 31) show that the N- and C-termini of its core domain are not far apart, so it might be possible to splice GFP into a noncritical exterior loop or domain boundary of the host protein. For example, residues 2–233 of GFP have been inserted between the last transmembrane segment and the long cytoplasmic tail of a Shaker potassium channel (100a).

## GFP AS AN ACTIVE INDICATOR

The rigid shell in GFP surrounding the chromophore enables it to be fluorescent and protects it from photobleaching but also hinders environmental sensitivity. Nevertheless, GFPs that act as indicators of their environment have been created by combinations of random and directed mutagenesis. The pH sensitivity of certain mutants and their potential application to measure organellar pH have already been mentioned. It is possible to engineer phosphorylation sites into GFP such that phosphorylation produces major changes in fluorescence under defined conditions (AB Cubitt, personal communication). The engineered fusion of GFP within the Shaker potassium channel is the first genetically encoded optical sensor of membrane potential (100a). Depolarization causes at most a 5% decrease in fluorescence with a time constant of approximately 85 ms, but both the amplitude and speed may well improve in future versions. But the most general way to make biochemically sensitive GFPs is to exploit fluorescence resonance energy transfer (FRET) between GFPs of different color. FRET is a quantum-mechanical phenomenon that occurs when two fluorophores are in molecular proximity ( $<100 \text{ \AA}$  apart) and the emission spectrum of one fluorophore, the donor, overlaps the excitation spectrum of the second fluorophore, the acceptor. Under these conditions, excitation of the donor can produce emission from the acceptor at the expense of the emission from the donor that would normally occur in the absence of the acceptor. Any biochemical signal that changes the distance between the fluorophores or relative orientation of their

transition dipoles will modulate the efficiency of FRET (101–103). Because FRET is a through-space effect, it is not necessary to perturb either GFP alone but rather only the linkage or spatial relationship between them. The potential utility of FRET between GFPs was the main motivation for the development of most of the mutations in Table 1. The change in ratio of acceptor to donor emissions is nearly ideal for cellular imaging and flow cytometry because the two emissions can be obtained simultaneously and their ratio cancels out variations in the absolute concentration of the GFPs, the thickness of the cell, the brightness of the excitation source, and the absolute efficiency of detection. Because the sample need be excited at only one wavelength, which should preferentially excite the donor, FRET is ideal for laser-scanning confocal microscopy and FACS (103). FRET also causes changes in donor fluorescence lifetime and bleaching rate (104), but detection of those signals either requires much more sophisticated instrumentation or is destructive.

### *Protease Action*

The simplest and first-demonstrated way to achieve and modulate FRET between GFPs was to fuse a blue-emitting (class 6) GFP mutant (i.e. a BFP) to a phenolate-containing (class 2) green GFP via an intervening protease-sensitive spacer (41, 105). The broad emission spectrum of the donor BFP, peaking at 447 nm, overlaps fairly well with the excitation spectrum of the class 2 GFP, peaking at 489 nm. Wild-type GFP would not be satisfactory, because the 383 nm used to excite the BFP would directly and efficiently excite the 395-nm excitation peak of wild-type GFP even in the absence of FRET. The tandem fusion exhibits FRET, which is then disrupted when a protease is added to cleave the spacer and let the GFPs diffuse apart. Heim & Tsien (41) used P4-3 and S65C or S65T and a trypsin- or enterokinase-sensitive 25-residue linker, and achieved a 4.6-fold increase in the ratio of blue to green emissions resulting from protease action. Control experiments verified that the two GFPs were unaffected by the proteases at the concentrations used, so the spectral change reflected cleavage of the linker. Mitra et al (105) used BFP5 (F64M, Y66H) and RSGFP4 with a Factor X<sub>a</sub>-sensitive linker and obtained a 1.9-fold increase in the analogous ratio. Although FRET-based assays for proteases are well known (106, 107), synthetic peptide substrates are limited in length and useful only in vitro. The special advantages of GFP-based constructs are that they could incorporate full-length protein substrates and could be expressed and assayed inside live cells or organisms.

### *Transcription Factor Dimerization*

A static homodimerization of the transcription factor Pit-1 has been detected by coexpression of BFP-Pit-1 and GFP-Pit-1 fusions in HeLa cells. Homodimerization is inherently more difficult than heterodimerization to demonstrate

by FRET, because at most 50% of the complexes will combine BFP- and GFP-labeled proteins, while nonproductive BFP-BFP and GFP-GFP complexes will each account for 25% of the homodimers. Nevertheless, careful spectral analysis indicated that homodimerization was detectable by FRET (108). Unfortunately, no modulation of the Pit-1 interaction or new biological conclusions were reported.

### *Ca<sup>2+</sup> Sensitivity*

The first dynamically responsive biochemical indicators based on GFP are Ca<sup>2+</sup> sensors, independently developed almost simultaneously by Romoser et al (109) and by Miyawaki et al (50). Romoser et al linked commercially available class 6 BFP and class 2 GFP mutants with a 26-residue spacer containing the calmodulin (CaM)-binding domain from avian smooth muscle myosin light chain kinase. This spacer allowed FRET to occur from the BFP to the GFP, perhaps because it was long and flexible enough for the two GFPs to dimerize. Addition of Ca<sup>2+</sup>-CaM disrupted FRET, presumably by binding to and straightening the linker so that the two GFPs were unable to dimerize. Such binding of Ca<sup>2+</sup>-CaM decreased the 505 nm emission by 65% and the ratio of 505- to 440-nm emissions by sixfold in vitro, an impressive spectral change for a reversible conformational change less drastic than proteolytic cleavage. The bacterially expressed recombinant protein was then microinjected into individual HEK-293 cells. In such intact cells, elevations of cytosolic free Ca<sup>2+</sup> produced much more modest decreases (5–10%) in 510-nm emission, which could be amplified to about 30% decreases if exogenous calmodulin was co-injected. Thus the response of the indicator in cells was limited by CaM availability, implying that the indicator is responsive to cellular Ca<sup>2+</sup>-CaM rather than Ca<sup>2+</sup> per se. Because the heterologously expressed protein had to be microinjected, the unique ability of GFP to be continuously synthesized by the target cell was not exploited, and only cytosolic signals could be monitored.

Miyawaki et al (50) fused BFP or class 5 cyan-fluorescent protein (CFP) to the N-terminus of CaM, and class 2 GFP or class 4 yellow-fluorescent protein (YFP) to the C-terminus of M13, the CaM-binding peptide from skeletal muscle myosin light chain kinase. The CFP-CaM and the M13-YFP could either be fused via two glycines (in which case all four protein domains were joined into a 76-kDa tandem chimera) or left separate. In either case, binding of Ca<sup>2+</sup> to the CaM caused it to grab the M13, thus increasing FRET, the opposite spectral effect from that of Romoser et al (109). By using GFPs with mutations to optimize mammalian expression, the indicators were bright enough to be introduced into cells by DNA transfection rather than protein microinjection. Because the four-domain chimeras were expressed in situ, they could readily be targeted to organelles such as the nucleus or endoplasmic reticulum by addition

**Table 3** Advantages and disadvantages of GFP-based  $\text{Ca}^{2+}$  indicators<sup>a</sup>

Advantages
Applicable to nearly all organisms; no need for ester permeation and hydrolysis
Can be targeted to specific tissues, cells, organelles, or proteins
Unlikely to diffuse well enough to blur spatial gradients
Modular construction is readily modified/improved by mutagenesis
Good optical properties: visible excitation, emission ratioing, high photostability
cDNAs or improved sequences are cheap to replicate and distribute
Should be generalizable to measure many bioactive species other than $\text{Ca}^{2+}$ , as long as a conformationally sensitive receptor is available
Disadvantages
Gene transfection required
The maximum change in emission ratio is currently less than for small-molecule dyes
The binding kinetics are somewhat slower
The CaM or M13 might have some additional biological activity

<sup>a</sup>GFP, green fluorescent proteins.

of appropriate targeting sequences.  $\text{Ca}^{2+}$  affinities were readily adjustable by mutation of the CaM. Thus free  $\text{Ca}^{2+}$  concentrations in the endoplasmic reticulum were measured to be 60–400  $\mu\text{M}$  in unstimulated cells, decreasing to 1–50  $\mu\text{M}$  in cells treated with  $\text{Ca}^{2+}$ -mobilizing agonists. Advantages and disadvantages of the GFP-based  $\text{Ca}^{2+}$  indicators (called cameleons) compared to conventional  $\text{Ca}^{2+}$  indicators are summarized in Table 3.

The constructs with separate CFP-CaM and M13-YFP proved that FRET between GFP mutants can dynamically monitor protein-protein interaction in single living cells. Binding of the two host proteins to each other brings their fused GFPs into proximity and enhances FRET. By comparison the mechanism of Romoser et al (109) requires that mutual binding must substantially change the distance between N- and C-terminii of at least one of the partners.

In principle the use of FRET offers some major advantages and disadvantages over other current methods for detecting protein-protein interaction (Table 4). The most unique advantages are the spatial and temporal resolution and the ability to observe the proteins in any compartment of the cell. The biggest disadvantage is that even in the absence of any protein interaction, a substantial background signal is present when illuminating at the donor's excitation maximum and observing at the acceptor's emission maximum. This background signal arises because the donor emission has a tail that extends into the acceptor's emission band, and the acceptor excitation has a tail that extends into the donor's excitation band. For these reasons, FRET is probably not a suitable method for detecting trace interactions or fishing for unknown partners but

**Table 4** Advantages and disadvantages of FRET between (GFPs) to monitor protein interactions.

---

---

**Advantages**

- Works in vitro and in living mammalian cells, not just yeast
- Can respond dynamically to posttranslational modifications
- Has high temporal (milliseconds) and spatial (submicron) resolution
- Interacting proteins can be anywhere in the cell and do not need to be sent to nucleus
- Degree of association can be quantified, if 0% and 100% binding can be established in situ
- Efficiency of FRET at 100% complexation gives some structural information

**Disadvantages of intermolecular FRET**

- Must express fusion proteins, in which host protein and GFPs must both remain functional
  - If GFPs are too far from each other ( $\gg 80 \text{ \AA}$ ) or unluckily oriented, FRET will fail
  - Even with no association, spectral overlap contributes some signal at the FRET wavelengths
  - Trace or rare interactions will be hard to detect
  - Need negative and positive controls, i.e. reference conditions of 0% and 100% association
  - Homodimerization is more difficult to monitor than heterodimerization
- 

is best used at a later stage when the two host proteins are molecularly well characterized and the detailed spatiotemporal dynamics of their interaction is to be determined in live cells.

*What Are the Best FRET Partners?*

The efficiency of FRET is given by the expression  $R_0^6/(R_0^6 + r^6)$ , where  $r$  is the actual distance between the centers of the chromophores and  $R_0$  is the distance at which FRET is 50% efficient.  $R_0$  depends on the quantum yield of the donor, the extinction coefficient of the acceptor, the overlap of the donor emission and acceptor excitation spectra, and the mutual orientation of the chromophores (102). The early attempts to obtain FRET between GFPs all used BFPs (class 6 mutants) as donors and class 2 (phenolate anion) GFPs as acceptors because these were the first available pairs with sufficiently distinct wavelengths. For such pairs,  $R_0$  is calculated to range from 40 to 43 Å. However, the poor extinction coefficients, quantum yields, and photostabilities of the BFPs have convinced us (50) that cyan mutants (class 5) are much better donors. The acceptor correspondingly must become a class 4 yellow mutant so that its excitation spectrum overlaps the donor emission as much as possible, whereas the two emissions remain as distinct as possible. Combinations of cyan donors with yellow acceptors have  $R_0$  values of 49–52 Å and are our currently preferred donor-acceptor pairs. So far, the highest value of  $R_0$  between two GFPs is 60 Å for class 3 mutant H9-40 as donor to Topaz, but unfortunately these mutants' emission spectra are too close to each other for good discrimination.

The above calculations have assumed that the GFPs are randomly oriented or tumbling with respect to one another, which is the conventional assumption

made in calculating  $R_0$  (102). If instead the mutual orientation of the two chromophores were the same as in the crystal structure for the wild-type dimer (31), the  $R_0$ s would be about 72% of the previously calculated values, for example, 35–37 Å for cyan-to-yellow FRET. For comparison, the actual distance  $r$  between the centers of the chromophores in the dimer is about 25 Å, which would predict that FRET would occur with about 90% efficiency in such a direct heterodimer between cyan and yellow mutants.

## OUTLOOK FOR FUTURE RESEARCH

Despite all that has been learned about how GFP works and how it can be exploited as a research tool, enormous challenges and opportunities remain. Listed below are some unanswered general questions about GFP that are among the most intriguing, excluding problems related to narrow applications in cell biology:

### *Cloning of Related GFPs*

What are the genetic sequences and structures of GFP homologs from bioluminescent organisms other than *Aequorea*? This information would illuminate the evolution of fluorescent proteins, reveal the essential conserved elements of the structure, and provide the genetic raw material for combinatorial mixing and matching to produce hybrid proteins with new phenotypes. *Renilla* GFP is the most obvious next cloning target, but even more bioluminescent organisms should be investigated.

### *Protein Folding and Chromophore Folding*

We need to know much more about how GFP folds into its  $\beta$ -barrel conformation and synthesizes its internal chromophore. Now that many of the steps have been kinetically resolved (23), the effect of mutations on each of the steps needs to be determined. The most informative mutants will not be the majority that completely prevent the formation of fluorescence, because those could act anywhere in the entire cascade including disruption of the final state. Instead, mutants or chaperonins that affect the rates but not the final extent of fluorescence development are likely to be most valuable. The molecular mechanism, kinetics, and byproducts of chromophore formation by  $O_2$  are particularly critical questions.

### *Altered Wavelengths of Fluorescence*

Yet longer wavelengths of excitation and emission than are currently available from the class 4 ( $\pi$ -stacked phenolate) mutants (Table 1) would be useful for multiple labels and reporters and to serve as resonance energy transfer acceptors.

For example, an increase in excitation maximum to 540–550 nm would permit efficient energy transfer from terbium chelates, whose millisecond excited-state lifetimes make them useful as energy transfer donors (110). The 560–570 nm emission from such longer-wavelength GFP mutants would also be distinct enough from the standard class 2 (phenolate) mutants to make such green-orange pairs useful as FRET partners. Another approach to improving FRET would be to reduce the emission bandwidth of the class 5 (tryptophan-based) cyan mutants and thereby improve the quantitative separation of cyan and yellow emissions. Emission spectral alterations should be most easily screened by fluorescence-activated cell sorting (FACS). The chemical structure of the red fluorescent species formed by intense illumination in anaerobic conditions (58) must be determined as the first step in making this extraordinary photochemical reaction more general and useful.

### *Altered Chemical and Photochemical Sensitivities*

The sensitivity of GFP spectra to environmental factors such as pH and past illumination is valuable if pH indication or photochemical tagging is desired but is a nuisance for most other applications. Therefore we need to understand the molecular mechanisms of such environmental modulations and to find mutations that enhance or eliminate those mechanisms. In many cases, it will be important to use screening methods that, unlike FACS, permit longitudinal comparison of individual cells or colonies before and after a chemical or actinic challenge. Digital imaging of colonies on plates (e.g. 111) is likely to be advantageous.

### *Fusions Other Than at N- or C-Terminus*

Almost all fusions of host proteins with GFP have been simple tandem fusions in which the C-terminus of one protein is genetically concatenated to the N-terminus of the other. Because not all such fusions work, general rules are needed in order to predict when fluorescence will be intact and when host protein function will be preserved. Sometimes neither order of simple concatenation produces functional chimeras. Could splicing of GFP into the middle of the host protein be made easier and more general? It might be helpful to engineer GFP to move its N- and C-termini as close to each other as possible, perhaps by addition of spacers or by circular permutation.

### *Alternatives to Fluorescence*

Chromophores can be harnessed to perform many functions other than fluorescence, such as phosphorescence (emission from the triplet state), generation of reactive oxygen species such as singlet oxygen or hydroxyl radical, and photochemical cleavage. Can GFP be engineered to do such tricks? Phosphorescence



typically gives lifetimes in microseconds rather than nanoseconds and therefore permits exploration of protein dynamics on longer time scales. Controlled generation of singlet oxygen can be useful to polymerize diaminobenzidine locally into a polymer visible by electron microscopy, so that the location of fluorophores can be verified at ultrastructural resolution (112). Laser pulses can be used to kill proteins within a few nanometers of a suitable chromophore that generates hydroxyl radicals or other reactive species (113). Photochemical cleavage is the basis of important methods to produce sudden changes in the concentration of signaling molecules (114). These techniques would be revolutionized if their crucial molecules could be synthesized or at least localized in situ under molecular biological control, in the same way as GFP. Of course, the rigid shell protecting the chromophore of GFP from the environment may intrinsically prevent even mutagenized GFPs from fulfilling such alternative functions, so that completely different proteins may need to be found or devised. Perhaps GFP will become just one prototype of a collection of genetically encoded, light-driven macromolecular reagents.

#### ACKNOWLEDGMENTS

I thank the many collaborators and colleagues who allowed me to cite their unpublished results or manuscripts in preparation. The Howard Hughes Medical Institute and the National Institutes of Health (NS27177) provided essential financial support.

Visit the *Annual Reviews* home page at  
<http://www.AnnualReviews.org>.

#### Literature Cited

1. Shimomura O, Johnson FH, Saiga Y. 1962. *J. Cell. Comp. Physiol.* 59:223–39
2. Johnson FH, Shimomura O, Saiga Y, Gershman LC, Reynolds GT, Waters JR. 1962. *J. Cell. Comp. Physiol.* 60:85–103
3. Morin JG, Hastings JW. 1971. *J. Cell. Physiol.* 77:313–18
4. Morise H, Shimomura O, Johnson FH, Winant J. 1974. *Biochemistry* 13:2656–62
5. Prendergast FG, Mann KG. 1978. *Biochemistry* 17:3448–53
6. Shimomura O. 1979. *FEBS Lett.* 104:220–22
7. Ward WW, Cody CW, Hart RC, Cormier MJ. 1980. *Photochem. Photobiol.* 31:611–15
8. Ward WW, Prentice HJ, Roth AF, Cody CW, Reeves SC. 1982. *Photochem. Photobiol.* 35:803–8
9. Ward WW, Bokman SH. 1982. *Biochemistry* 21:4535–40
10. Prasher DC, Eckenrode VK, Ward WW, Prendergast FG, Cormier MJ. 1992. *Gene* 111:229–33
11. Chalfie M, Tu Y, Euskirchen G, Ward WW, Prasher DC. 1994. *Science* 263:802–5
12. Inouye S, Tsuji FI. 1994. *FEBS Lett.* 341:277–80
13. Ward WW. 1979. In *Photochemical and Photobiological Reviews*, ed. KC Smith, 4:1–57. New York: Plenum
14. Ward WW, Cormier MJ. 1979. *J. Biol. Chem.* 254:781–88
15. Lee J, Gibson BG, O’Kane DJ, Kohnle A, Bacher A. 1992. *Eur. J. Biochem.*

- 210:711–19
16. Macheroux P, Schmidt KU, Steinerstauch P, Ghisla S. 1987. *Biochem. Biophys. Res. Commun.* 146:101–6
  17. Glazer AN. 1989. *J. Biol. Chem.* 264:1–4
  18. Song P-S, Koka P, Prézélin BB, Haxo FT. 1976. *Biochemistry* 15:4422–27
  19. Tsien RY, Prasher DC. 1997. In *GFP: Green Fluorescent Protein Strategies and Applications*, ed. M Chalfie, S Kain. New York: Wiley & Sons
  20. Cody CW, Prasher DC, Westler WM, Prendergast FG, Ward WW. 1993. *Biochemistry* 32:1212–18
  21. Heim R, Prasher DC, Tsien RY. 1994. *Proc. Natl. Acad. Sci. USA* 91:12501–4
  22. Cubitt AB, Heim R, Adams SR, Boyd AE, Gross LA, Tsien RY. 1995. *Trends Biochem. Sci.* 20:448–55
  23. Reid BG, Flynn GC. 1997. *Biochemistry* 36:6786–91
  24. Inouye S, Tsuji FI. 1994. *FEBS Lett.* 351:211–14
  25. Heim R, Cubitt AB, Tsien RY. 1995. *Nature* 373:663–64
  26. Kojima S, Hirano T, Niwa H, Ohashi M, Inouye S, Tsuji FL. 1997. *Tetrahedron Lett.* 38:2875–78
  27. Wright HT. 1991. *Crit. Rev. Biochem. Mol. Biol.* 26:1–52
  28. Rizzuto R, Brini M, DeGiorgi F, Rossi R, Heim R, et al. 1996. *Curr. Biol.* 6:183–88
  29. Perozzo MA, Ward KB, Thompson RB, Ward WW. 1988. *J. Biol. Chem.* 263:7713–16
  30. Ormö M, Cubitt AB, Kallio K, Gross LA, Tsien RY, Remington SJ. 1996. *Science* 273:1392–95
  31. Yang F, Moss LG, Phillips GN Jr. 1996. *Nat. Biotechnol.* 14:1246–51
  32. Brejc K, Sixma TK, Kitts PA, Kain SR, Tsien RY, et al. 1997. *Proc. Natl. Acad. Sci. USA* 94:2306–11
  33. Palm GJ, Zdanov A, Gaitanaris GA, Stauber R, Pavlakis GN, Wlodawer A. 1997. *Nat. Struct. Biol.* 4:361–65
  34. Wachter RM, King BA, Heim R, Kallio K, Tsien RY, et al. 1997. *Biochemistry* 36:9759–65
  - 34a. Phillips GN Jr. 1997. *Curr. Opin. Struct. Biol.* 7:821–27
  35. Dopf J, Horiagon TM. 1996. *Gene* 173:39–44
  36. Chattoraj M, King BA, Bublitz GU, Boxer SG. 1996. *Proc. Natl. Acad. Sci. USA* 93:8362–67
  37. Yokoe H, Meyer T. 1996. *Nat. Biotechnol.* 14:1252–56
  38. Lim CR, Kimata Y, Oka M, Nomaguchi K, Kohno K. 1995. *J. Biochem.* 118:13–17
  39. Kaether C, Gerdes HH. 1995. *FEBS Lett.* 369:267–71
  40. Cramer A, Whitehorn EA, Tate E, Stemmer WPC. 1996. *Nat. Biotechnol.* 14:315–19
  41. Heim R, Tsien RY. 1996. *Curr. Biol.* 6:178–82
  42. Kahana J, Silver P. 1996. In *Current Protocols in Molecular Biology*, ed. FM Ausabel, R Brent, RE Kingston, DD Moore, JG Seidman, et al, 9(7):22–28 New York: Wiley & Sons
  43. Patterson GH, Knobel SM, Sharif WD, Kain SR, Piston DW. 1997. *Biophys. J.* 73:2782–90
  44. Cubitt AB, Heim R, Woollenweber LA. 1997. *Methods Cell Biol.* In press
  45. Ward WW. 1997. In *Green Fluorescent Protein: Properties, Applications, and Protocols*, ed. M Chalfie, S Kain. New York: John Wiley & Sons
  46. Delagrave S, Hawtin RE, Silva CM, Yang MM, Youvan DC. 1995. *Bio-Technology* 13:151–14
  47. Cormack BP, Valdivia RH, Falkow S. 1996. *Gene* 173:33–38
  48. Cheng LZ, Fu J, Tsukamoto A, Hawley RG. 1996. *Nat. Biotechnol.* 14:606–9
  49. Ehrig T, O’Kane DJ, Prendergast FG. 1995. *FEBS Lett.* 367:163–66
  50. Miyawaki A, Llopis J, Heim R, McCaffery JM, Adams JA, et al. 1997. *Nature* 388:882–87
  51. Wu C, Liu HZ, Crossen R, Gruenwald S, Singh S. 1997. *Gene* 190:157–62
  52. Niwa H, Inouye S, Hirano T, Matsuno T, Kojima S, et al. 1996. *Proc. Natl. Acad. Sci. USA* 93:13617–22
  53. Voityuk AA, Michel-Beyerle ME, Röscher N. 1997. *Chem. Phys. Lett.* 272:162–67
  54. Xu C, Zipfel W, Shear JB, Williams RM, Webb WW. 1996. *Proc. Natl. Acad. Sci. USA* 93:10763–68
  55. Niswender KD, Blackman SM, Rohde L, Magnuson MA, Piston DW. 1995. *J. Microsc.* 180:109–16
  56. Potter SM, Wang C-M, Garrity PA, Fraser SE. 1996. *Gene* 173:25–31
  57. Bokman SH, Ward WW. 1981. *Biochem. Biophys. Res. Commun.* 101:1372–80
  58. Elowitz MB, Surette MG, Wolf E, Stock J, Leibler S. 1997. *Curr. Biol.* 7:809–12
  59. Swaminathan KS, Hoang CP, Verkman AS. 1997. *Biophys. J.* 72:1900–7
  60. Subramanian K, Meyer T. 1997. *Cell* 89:963–71

61. Dickson RM, Cubitt AB, Tsien RY, Moerner WE. 1997. *Nature* 388:355–58
62. Haseloff J, Siemering KR, Prasher DC, Hodge S. 1997. *Proc. Natl. Acad. Sci. USA* 94:2122–27
63. Zolotukhin S, Potter M, Hauswirth WW, Guy J, Muzyczka N. 1996. *J. Virol.* 70: 4646–54
64. Yang T-T, Cheng L, Kain SR. 1996. *Nucleic Acids Res.* 24:4592–93
65. Cormack BP, Bertram G, Egerton M, Gow NAR, Falkow S, Brown AJP. 1997. *Microbiology* 143:303–11
66. Kozak M. 1989. *J. Cell Biol.* 108:229–41
67. Kahn TW, Beachy RN, Falk MM. 1997. *Curr. Biol.* 7:R207–8
68. Weissman JS, Rye HS, Fenton WA, Beechem JM, Horwich AL. 1996. *Cell* 84:481–90
69. Makino Y, Amada K, Taguchi H, Yoshida M. 1997. *J. Biol. Chem.* 272:12468–74
70. Ikawa M, Kominami K, Yoshimura Y, Tanaka K, Nishimune Y, Okabe M. 1995. *Dev. Growth Differ.* 37:455–59
71. Zernicka-Goetz M, Pines J, Hunter SM, Dixon JPC, Siemering KR, et al. 1997. *Development* 124:1133–37
72. Chiochetti A, Tolosano E, Hirsch E, Silengo L, Altruda F. 1997. *Biochim. Biophys. Acta* 1352:193–202
73. Gagneten S, Le Y, Miller J, Sauer B. 1997. *Nucleic Acids Res.* 25:3326–31
74. Takada T, Iida K, Awaji T, Itoh K, Takahashi R, et al. 1997. *Nat. Biotechnol.* 15:458–61
75. Ikawa M, Kominami K, Yoshimura Y, Tanaka K, Nishimune Y, Okabe M. 1995. *FEBS Lett.* 375:125–28
76. Amsterdam A, Lin S, Moss LG, Hopkins N. 1996. *Gene* 173:99–103
77. Muldoon RR, Levy JP, Kain SR, Kitts PA, Link CJJ. 1997. *BioTechniques* 22: 162–67
78. Zhang GH, Gurtu V, Kain SR. 1996. *Biochem. Biophys. Res. Commun.* 227: 707–11
79. Gervaix A, West D, Leoni LM, Richman DD, Wong-Staal F, Corbeil J. 1997. *Proc. Natl. Acad. Sci. USA* 94:4653–58
80. Anderson MT, Tjioe IM, Lorincz MC, Parks DR, Herzenberg LA, Nolan GP. 1996. *Proc. Natl. Acad. Sci. USA* 93: 8508–11
81. Mosser DD, Caron AW, Bourget L, Jolicoeur P, Massie B. 1997. *BioTechniques* 22:150–61
82. Shelby RD, Hahn KM, Sullivan KF. 1996. *J. Cell Biol.* 135:545–57
83. Zlokarnik G, Negulescu PA, Knapp TE, Santiso-Mere D, Burres N, et al. 1998. *Science* 279:84–88
84. Marshall J, Molloy R, Moss GWJ, Howe JR, Hughes TE. 1995. *Neuron* 14:211–15
85. Barak LS, Ferguson SSG, Zhang J, Martenson C, Meyer T, Caron MG. 1997. *Mol. Pharmacol.* 51:177–84
86. Moriyoshi K, Richards LJ, Akazawa C, O'Leary DDM, Nakanishi S. 1996. *Neuron* 16:255–60
87. Hanakam F, Albrecht R, Eckerskorn C, Matzner M, Gerisch G. 1996. *EMBO J.* 15:2935–43
88. Grebenok RJ, Pierson E, Lambert GM, Gong F-C, Afonso CL, et al. 1997. *Plant J.* 11:573–86
89. DeGiorgi F, Brini M, Bastianutto C, Marsault R, Montero M, et al. 1996. *Gene* 173:113–17
90. Corbett AH, Koepf DM, Schlenstedt G, Lee MS, Hopper AK, Silver P. 1995. *J. Cell Biol.* 130:1017–26
91. Carey KL, Richards SA, Lounsbury KM, Macara IG. 1996. *J. Cell Biol.* 133: 985–96
92. Chatterjee S, Stochaj U. 1996. *BioTechniques* 21:62–63
93. Presley JF, Cole NB, Schroer TA, Hirschberg K, Zaal KJM, Lippincott-Schwartz J. 1997. *Nature* 389:81–85
94. Lang T, Wacker I, Steyer J, Kaether C, Wunderlich I, et al. 1997. *Neuron* 18:857–63
95. Murray AW, Kirschner MW. 1989. *Science* 246:614–21
96. Yano M, Kanazawa M, Terada K, Nam-chai C, Yamaizumi M, et al. 1997. *J. Biol. Chem.* 272:8459–65
97. Wiemer EAC, Wenzel T, Deerinck TJ, Ellisman MH, Subramani S. 1997. *J. Cell Biol.* 136:71–80
98. Cowles CR, Odorizzi G, Payne GS, Emr SD. 1997. *Cell* 91:109–18
99. Maniak M, Rauchenberger R, Albrecht R, Murphy J, Gerisch G. 1995. *Cell* 83: 915–24
100. Straight AF, Marshall WF, Sedat JW, Murray AW. 1997. *Science* 277:574–78
- 100a. Siegel MS, Isacoff EY. 1997. *Neuron* 19:735–41
101. Stryer L. 1978. *Annu. Rev. Biochem.* 47: 819–46
102. Lakowicz JR. 1983. *Principles of Fluorescence Spectroscopy*. New York: Plenum

103. Tsien RY, Bacsikai BJ, Adams SR. 1993. *Trends Cell Biol.* 3:242–45
104. Jovin TM, Arndt-Jovin DJ. 1989. *Annu. Rev. Biophys. Biophys. Chem.* 18:271–308
105. Mitra RD, Silva CM, Youvan DC. 1996. *Gene* 173:13–17
106. Krafft GA, Wang GT. 1994. *Methods Enzymol.* 241:70–86
107. Knight CG. 1995. *Methods Enzymol.* 248:18–34
108. Periasamy A, Kay SA, Day RN. 1997. In *Functional Imaging and Optical Manipulation of Living Cells, Proc. SPIE 2983*, ed. DL Farkas, BJ Tromberg. Bellingham, WA: SPIE
109. Romoser VA, Hinkle PM, Persechini A. 1997. *J. Biol. Chem.* 272:13270–74
110. Selvin PR. 1996. *IEEE J. Sel. Top. Quant. Electron.* 2:1077–87
111. Youvan DC, Goldman ER, Delgrave S, Yang MM. 1995. *Methods Enzymol.* 246:732–48
112. Deerinck TJ, Martone ME, Lev-Ram V, Green DPL, Tsien RY, et al. 1994. *J. Cell Biol.* 126:901–10
113. Linden KG, Liao JC, Jay DG. 1992. *Biophys. J.* 61:956–62
114. Adams SR, Tsien RY. 1993. *Annu. Rev. Physiol.* 55:755–84



## CONTENTS

An Accidental Biochemist, <i>Edwin G. Krebs</i>	0
HIV-1: Fifteen Proteins and an RNA, <i>Alan D. Frankel and John A. T. Young</i>	1
Sphingolipid Functions in <i>Saccharomyces Cerevisiae</i> : Comparison to Mammals, <i>Robert C. Dickson</i>	27
Transporters of Nucleotide Sugars, ATP, and Nucleotide Sulfate in the Endoplasmic Reticulum and Golgi Apparatus, <i>Carlos B. Hirschberg, Phillips W. Robbins, and Claudia Abeijon</i>	49
Ribonucleotide Reductases, <i>A. Jordan and P. Reichard</i>	71
Modified Oligonucleotides: Synthesis and Strategy for Users, <i>Sandeep Verma and Fritz Eckstein</i>	99
The Molecular Control of Circadian Behavioral Rhythms and Their Entrainment in <i>Drosophila</i> , <i>Michael W. Young</i>	135
Ribonuclease P: Unity and Diversity in a tRNA Processing Ribozyme, <i>Daniel N. Frank and Norman R. Pace</i>	153
Base Flipping, <i>Richard J. Roberts and Xiaodong Cheng</i>	181
The Caveolae Membrane System, <i>Richard G. W. Anderson</i>	199
How Cells Respond to Interferons, <i>George R. Stark, Ian M. Kerr, Bryan R. G. Williams, Robert H. Silverman, and Robert D. Schreiber</i>	227
Nucleocytoplasmic Transport: The Soluble Phase, <i>Iain W. Mattaj and Ludwig Englmeier</i>	265
Role of Small G Proteins in Yeast Cell Polarization and Wall Biosynthesis, <i>Enrico Cabib, Jana Drgonová, and Tomás Drgon</i>	307
RNA Localization in Development, <i>Arash Bashirullah, Ramona L. Cooperstock, and Howard D. Lipshitz</i>	335
Biochemistry and Genetics of von Willebrand Factor, <i>J. Evan Sadler</i>	395
The Ubiquitin System, <i>Avram Hershko and Aaron Ciechanover</i>	425
Phosphoinositide Kinases, <i>David A. Fruman, Rachel E. Meyers, and Lewis C. Cantley</i>	481
The Green Fluorescent Protein, <i>Roger Y. Tsien</i>	509
Alteration of Nucleosome Structure as a Mechanism of Transcriptional Regulation, <i>J. L. Workman, and R. E. Kingston</i>	545
Structure and Function in GroEL-Mediated Protein Folding, <i>Paul B. Sigler, Zhaohui Xu, Hays S. Rye, Steven G. Burston, Wayne A. Fenton, and Arthur L. Horwich</i>	581
Matrix Proteoglycans: From Molecular Design to Cellular Function, <i>Renato V. Iozzo</i>	609
G Protein Coupled Receptor Kinases, <i>Julie A. Pitcher, Neil J. Freedman, and Robert J. Lefkowitz</i>	653
Enzymatic Transition States and Transition State Analog Design, <i>Vern L. Schramm</i>	693

The DNA Replication Fork in Eukaryotic Cells, <i>Shou Waga and Bruce Stillman</i>	721
TGF-beta Signal Transduction, <i>J. Massagué</i>	753
Pathologic Conformations of Prion Proteins, <i>Fred E. Cohen and Stanley B. Prusiner</i>	793
The AMP-Activated/SNF1 Protein Kinase Subfamily: Metabolic Sensors of the Eukaryotic Cell?, <i>D. Grahame Hardie, David Carling, and Marian Carlson</i>	821